Salmonella enterica serovar Typhimurium chitinases modulate the intestinal glycome and promote small intestinal invasion.

Jason R Devlin[1], William Santus[1], Jorge Mendez[1], Wenjing Peng[2], Aiying Yu[2], Junyao Wang[2], Xiomarie Alejandro-Navarreto[1], Kaitlyn Kiernan[1], Manmeet Singh[3], Peilin Jiang[2], Yehia Mechref[2], and Judith Behnsen[1*]

[1]Department of Microbiology and Immunology, University of Illinois Chicago, Chicago, Illinois, United States of America

[2]Department of Chemistry and Biochemistry, Texas Tech University, Lubbock, Texas, United States of America

[3]Department of Pathology, University of Illinois Chicago, Chicago, Illinois, United States of America

Short Title: *Salmonella* chitinases modulate the intestinal glycome.

*Corresponding Author: jbehnsen@uic.edu (JB)

Funding: Funds provided by the National Institutes of Health (1R01AI143641 to JB and 1R01GM112490 to YM) and the Department of Microbiology at the University of Illinois Chicago (to JB). The funders had no role in study design, data collection and analysis, decision to publish, or preparation of the manuscript.

Data availability: Glycome analysis data set is available in the GlycoPOST repository via the accession number GPST000225. The preview page can be accessed through: https://glycopost.glycosmos.org/preview/2086580268617c0c826fa8c with pin code 6083. All other relevant data is present within this manuscript.

Abstract

Salmonella enterica serovar Typhimurium (*Salmonella*) is one of the leading causes of food-borne illnesses worldwide. To colonize the gastrointestinal tract, *Salmonella* produces multiple virulence factors that facilitate cellular invasion. Chitinases have been recently emerging as virulence factors for various pathogenic bacterial species and the *Salmonella* genome contains two annotated chitinases: *STM0018* (*chiA*) and *STM0233*. However, the role of these chitinases during *Salmonella* pathogenesis is unknown. The putative chitinase STM0233 has not been studied previously and only limited data exists on ChiA. Chitinases typically hydrolyze chitin polymers, which are absent in vertebrates. However, *chiA* expression was detected in infection models and purified ChiA cleaved carbohydrate subunits present on mammalian surface glycoproteins, indicating a role during pathogenesis. Here, we demonstrate that expression of *chiA* and *STM0233* is upregulated in the mouse gut and that both chitinases facilitate epithelial cell adhesion and invasion. *Salmonella* lacking both chitinases showed a 70% reduction in invasion of small intestinal epithelial cells *in vitro*. In a gastroenteritis mouse model, chitinase-deficient *Salmonella* strains were also significantly attenuated in the invasion of small intestinal tissue. This reduced invasion resulted in significantly delayed *Salmonella* dissemination to the spleen and the liver, but chitinases were not required for systemic survival. The invasion defect of the chitinase-deficient strain was rescued by the presence of wild-type *Salmonella*, suggesting that chitinases are secreted. By analyzing *N*-linked glycans of small intestinal cells, we identified specific *N*-acetylglucosamine-containing glycans as potential extracellular targets of *Salmonella* chitinases. This analysis also revealed differential abundance of Lewis X-containing glycans that is likely a result of host cell modulation due to the detection of *Salmonella* chitinases. Similar glycomic changes elicited by chitinase deficient strains indicate functional redundancy of the chitinases. Overall, our results demonstrate that *Salmonella* chitinases contribute to intestinal adhesion and invasion through modulation of the host glycome.

Author Summary

Salmonella Typhimurium infection is one of the leading causes of food-borne illnesses worldwide. In order for *Salmonella* to effectively cause disease, it has to invade the epithelial cells lining the intestinal tract. This invasion step allows *Salmonella* to replicate efficiently, causing further tissue damage and inflammation. In susceptible patients, *Salmonella* can spread past the intestines and infect peripheral organs. It is essential to fully understand the invasion mechanism used by *Salmonella* to design better treatments for infection. Here, we demonstrate that the two chitinases produced by *Salmonella* are involved in this invasion process. We show that *Salmonella* chitinases interact with surface glycans of intestinal epithelial cells and promote adhesion and invasion. Using a mouse infection model, we show that *Salmonella* chitinases are required for the invasion of the small intestine and enhance the dissemination of *Salmonella* to other organs. This study reveals an additional mechanism by which *Salmonella* invades and causes infection.

Introduction

As a food-borne pathogen, *Salmonella* colonizes the gastrointestinal tract causing self-limiting gastroenteritis. A critical step in the infection cycle of *Salmonella* is the invasion of intestinal epithelial cells via the type-3 secretion system-1 (T3SS-1) [1]. Once inside, *Salmonella* hyper-replicates and triggers pyroptosis of the intestinal epithelial cell, releasing newly formed bacterial cells back into the intestinal lumen, exacerbating infection [2]. Immuno-compromised individuals are more susceptible to infection due to the ability of *Salmonella* to breach the epithelial barrier and disseminate to peripheral organs, causing a systemic infection [3]. *Salmonella* expresses a variety of virulence factors that promote this pathogenic lifestyle. These provide functions ranging from aiding in the adhesion to and invasion of intestinal epithelial cells, promoting intracellular survival, and modulating the host immune response [4–6]. Many of these virulence factors have been studied in detail, while others are continuously being discovered. Two chitinases present in

the genome of *Salmonella* LT2, STM0018 (ChiA) and STM0233, have been recently proposed as potential virulence factors [7]. Our study uses the ATCC 14028 strain of *Salmonella*, which has the genomic identifier *STM14_0022* and *STM14_0275* for *chiA* and *STM0233*, respectively. For the sake of consistency, we will use the LT2 nomenclature to refer to these chitinases.

The main function of chitinases is the hydrolysis of chitin polymers into *N*-acetyl glucosamine (GlcNAc) oligomers [8]. Chitin is a component of the cuticle of insects and crustaceans and is a part of the fungal cell wall, making it the second most abundant biopolymer in nature. Despite chitin's prevalence, it is absent in mammalian species [8]. However, chitinases can also demonstrate catalytic activity towards other GlcNAc-containing polysaccharides, such as peptidoglycan [9]. This observation indicates that chitinases may interact with other biologically relevant polysaccharides to serve alternative roles. Interestingly, chitinases and chitin-binding proteins, which are similar to chitinases but lack catalytic activity, are emerging as virulence factors for various pathogenic bacterial species. *Legionella pneumophila* expresses a chitinase that shows catalytic activity towards mucins and is required for colonization of the lungs [10,11]. The intestinal pathogen *Listeria monocytogenes* produces a chitinase that modulates inducible nitric oxide synthase (iNOS) expression to facilitate colonization of the liver and spleen [12,13]. *Vibrio cholerae* produces a chitinase that degrades and allows the utilization of intestinal mucins as a carbon source [14]. *V. cholerae* also produces a chitin-binding protein that adheres to mucins to promote gastrointestinal colonization [14,15]. Both Adherent-Invasive *Escherichia coli* (AIEC) and *Serratia marcescens* produce a chitinase and a chitin-binding protein, respectively, that contribute to the adhesion to intestinal epithelial cells [16,17]. A mammalian chitin-binding protein, Chitinase 3 like 1, has already been implicated in *Salmonella* infection by promoting the invasion of colonic epithelial cells *in vitro* and intestinal colonization and dissemination *in vivo* [18]. These previous studies indicate that the chitinases encoded by *Salmonella* have the potential to contribute to human infection.

Despite the clear interest in the roles of chitinases during infection, *Salmonella* chitinases have yet to be studied in detail, and their roles in gastrointestinal infection are still unknown. The putative chitinase STM0233 has not been studied experimentally, and its expression, enzymatic activity, and role during infection are entirely unknown. The expression of *chiA* has been detected during infection of epithelial cells, murine macrophages, and the gastrointestinal system of chickens [19–21]. The enzymatic activity of ChiA has been partially elucidated. As expected, ChiA shows *in vitro* hydrolytic activity towards chitin. However, ChiA also cleaves *N*-acetyllactosamine (LacNAc) [22,23], a common component of surface glycoproteins of intestinal epithelial cells. *Salmonella* chitinases might therefore represent glycoside hydrolases that have flexible specificity and interact with the intestinal glycome. In many surface glycoproteins, LacNAc masks the underlying mannose subunits [24]. Exposing these mannose residues is potentially important for *Salmonella* pathogenesis. An increase of high-mannose glycans was previously shown to increase invasion of intestinal epithelial cells *in vitro* [25,26]. *Salmonella* also produces a type 1 fimbria (FimH) that binds mannose subunits on surface glycoproteins to facilitate adhesion to host cells [27]. Therefore, we hypothesized that *Salmonella* chitinases are remodeling the intestinal glycome by removing LaNAc residues to expose mannose residues that facilitate the adhesion to and invasion of intestinal epithelial cells. Here, we demonstrate that both *Salmonella* chitinases are required to adhere to and invade intestinal epithelial cells *in vitro*. In a mouse model, chitinases facilitated small intestinal cell invasion, which contributed to *Salmonella* dissemination to peripheral organs. Presence of *Salmonella* chitinases resulted in specific changes in the abundance of GlcNAc-containing *N*-linked surface glycans, indicating that chitinases cleave these GlcNAc residues. *Salmonella* chitinase also stimulated host cells to upregulate Lewis X-containing glycans and other complex glycan species.

Results

Salmonella chitinases are required for intestinal epithelial cell adhesion and invasion.

Since there are no experimental studies on STM0233 and only limited studies of ChiA in the current literature [22,23], we set out to determine the roles of these two chitinases during *Salmonella* infection. We first confirmed that both chitinases are expressed by *Salmonella in vitro.* The expression of *STM0233* and *chiA* mRNA was detectable by RT-qPCR. Wild-type (WT) *Salmonella* expressed both chitinases under growth conditions relevant to our *in vitro* studies (LB broth and DMEM/F12 + 10% FBS) (Fig. 1A). We observed a 2-fold upregulation of *STM0233* in DMEM/F12, but a similar expression of *chiA* across both media (Fig. 1A). We generated single- and double-deletion strains lacking the chitinase encoding genes and confirmed that the strains have similar growth kinetics as WT in rich medium (Fig. S1A). One potential role for *Salmonella* chitinases is the degradation and utilization of dietary chitin as a carbon source. We thus performed growth curves in minimal media supplemented with colloidal chitin but found no difference in the growth of strains lacking chitinases compared to WT (Fig. S1B). The lack of a growth defect for the chitinase-deficient strains indicates that *Salmonella* chitinases are not involved in utilizing chitin as a carbon source.

ChiA's activity towards LacNAc *in vitro* indicates that this chitinase has the potential to interact with surface glycoproteins of intestinal epithelial cells [22,23]. Interactions with surface glycoproteins have been previously shown to promote *Salmonella* invasion [25–27]. We therefore hypothesized that *Salmonella* chitinases facilitate the invasion of intestinal epithelial cells to promote infection. We assessed the capabilities of the chitinase-deficient strains to invade epithelial cells of the small intestine (IPEC-1) and colon (T-84) by performing a gentamicin protection assay. An *invA* deletion strain was used as a negative control, as it lacks expression of a functional T3SS-1, which is required to invade this cell type [28]. *Salmonella* strains deficient in only one chitinase showed a trend towards reduced invasion of colonic cells, whereas the strain deficient in both chitinases (*ΔSTM0233 ΔchiA*) showed a highly significant >70% reduction in invasion compared to WT (Fig. 1B). In the small intestinal epithelial cell line (IPEC-1), invasion

151 deficiencies of *Salmonella* strains lacking chitinases were even more evident. Here, strains
152 deficient in only one chitinase also showed >70% reduction in invasion, similar to the double-
153 chitinase deletion strain (Fig. 1C). The complementation of the deleted chitinase genes restored
154 invasion of the chitinase-deficient strains (Fig. S2). Therefore, both STM0233 and ChiA contribute
155 to the invasion of intestinal epithelial cells, and deletion of either chitinase seems to have a greater
156 effect on small intestinal invasion than colonic invasion.

157 Invasion of intestinal epithelial cells by *Salmonella* requires successful adhesion and the
158 deployment of the T3SS [29,30]. We therefore investigated whether chitinases contribute directly
159 to invasion or if their primary role is influencing adhesion. Intestinal epithelial cells were incubated
160 with cytochalasin D prior to and during infection to inhibit the actin rearrangement required for
161 *Salmonella* invasion. Cytochalasin D treatment completely blocked the invasion of colonic and
162 small intestinal cells (Fig. S3A, B). The *invA* deletion strain was used as a negative control since
163 the T3SS-1 is known to contribute to the stable adhesion to epithelial cells [31,32]. In colonic
164 epithelial cells, the *ΔSTM0233* strain showed a 33% reduction in adhesion compared to WT (Fig.
165 1D), indicating a potentially more significant role for STM0233 in adhesion than ChiA. The double-
166 deletion strain also showed a trend toward reduced adhesion ($p=0.0698$; Fig. 1D). In the small
167 intestinal cell line, the double-deletion strains showed a 50% reduction in adhesion (Fig. 1E),
168 similar to the observed 70% reduced invasion (Fig. 1C). Although chitinases seem to play a partial
169 role in contributing to colonic adhesion, both chitinases significantly contributed to the adhesion
170 to small intestinal cells.

171

172 **_Salmonella_ chitinases are required for invasion and colonization of the small intestines _in_**
173 ***vivo*.**

Given the significant role of chitinases as invasion factors for epithelial cells *in vitro*, we next explored if chitinases contribute to *Salmonella* pathogenicity *in vivo*. We used a streptomycin-pretreatment mouse model (Fig. 2A), in which C57BL/6 mice were treated with streptomycin 24 h prior to infection to promote *Salmonella* colonization of the intestinal tract and to allow *Salmonella* to trigger intestinal inflammation similar to human infection [33]. We first tested if expression of chitinase genes was changed in colonic luminal samples collected 48 hours post-infection (hpi) compared to LB. Expression of both *STM0233* and *chiA* was significantly upregulated *in vivo* (Fig. 2B). We further examined *Salmonella* invasion of the ileum and colon by performing a gentamicin protection assay on intestinal tissue and determined luminal colonization levels. The chitinase-deficient strains displayed markedly reduced invasion of ileal tissue at 48 hpi, with the double-deletion strain showing a 10-fold invasion defect compared to *Salmonella* WT (Fig. 2C). Simultaneously, chitinase-deficient strains also showed a defect in the colonization of the lumen of the ileum (Fig. 2C). Surprisingly, there was no defect in the ability of the chitinase-deficient strains to invade colonic tissue or colonize the colon at 48 hpi (Fig 2D). Consistent with this finding, chitinase-deficient strains did not show decreased colonization in fecal samples collected throughout infection (Fig. 2D). The *in vivo* invasion defect is therefore specific to the small intestines, despite the invasion defect observed during *in vitro* infection of colonic epithelial cells (Fig. 1B).

Salmonella chitinases are required for dissemination during the early stages of gastrointestinal infection but are dispensable during systemic infection.

Early during infection, *Salmonella* specifically targets M cells and invades Peyer's patches [34]. *Salmonella* is then transported to the mesenteric lymph nodes by antigen-presenting cells and eventually colonizes the spleen and liver, entering systemic circulation [35]. We therefore investigated the ability of the chitinase-deficient strains to disseminate to peripheral organs during

199 infection. Both the *chiA* (14-fold) and the double-deletion strain (50-fold) showed significantly
200 reduced colonization of the spleen 48 hpi compared to WT *Salmonella* (Fig. 3A). Strikingly, for all
201 but one mouse, the double-chitinase deletion strain did not colonize the liver to detectable levels,
202 in contrast to WT *Salmonella* (Fig. 3A). This colonization defect may be due to a direct role of
203 chitinases for *Salmonella* survival at systemic sites. To rule out this possibility, we administered
204 *Salmonella* directly into the peritoneum. Without the requirement of intestinal invasion, chitinase-
205 deficient strains were able to colonize the spleen and the liver to a similar extent as WT (Fig. 3B).
206 These results indicate that chitinase-mediated invasion of the intestines leads to an increase in
207 dissemination. No colonization defect was detected in the Peyer's patches or mesenteric lymph
208 nodes at 48 hours post-gastrointestinal infection (Fig 3A). These sites are the first that *Salmonella*
209 disseminates to during infection [35]. An initial defect in the colonization of the Peyer's patches or
210 mesenteric lymph nodes due to lower gastrointestinal invasion might thus be masked by bacterial
211 replication.

212 The hypothesis that chitinases are mediators during the early stages of infection is supported by
213 data from an extended infection mouse model (Fig. S4A). When mice were infected for 96 h, both
214 WT and chitinase-deficient strains showed similar invasion and colonization of the ileum (Fig.
215 S4B). Chitinase-deficient strains were also not defective in their ability to colonize the colon or
216 disseminate to the Peyer's patches, mesenteric lymph nodes, spleen, or liver (Fig. S4C-D). Our
217 findings thus far show that chitinases are required during early infection but are dispensable for
218 survival at systemic sites and during later stages of infection once *Salmonella* has fully
219 established colonization.

220

221 **_Salmonella_ chitinases are not involved in modulating the innate immune response.**

Based on the ability of the chitinase produced by *Listeria monocytogenes*, ChiA, to downregulate the expression of inducible nitric oxide synthase (iNOS) as a mechanism to promote colonization of the liver and spleen [12], we set out to explore if *Salmonella* chitinases interact with the immune system in a similar manner. We collected cecal tissue from mice infected with WT or chitinase-deficient strains for 48h and analyzed the expression of a panel of genes that are known to be involved in the immune response to *Salmonella* infection [6,36]. We found no changes in the expression of *Nos2, Duox2, Cxcl1, Ifng, Il6, Il22, Il23, S100a9* (encoding a subunit of the antimicrobial protein calprotectin), *Lcn2, IL1b,* or *Tnf* in mice infected with chitinase-deficient strains compared to WT infected mice (Fig. 4A-K). We detected a 2-fold upregulation of *Il17* in mice infected with chitinase-deficient strains (Fig. 4L). The biological relevance of this differential expression is unclear, as there are no changes in upstream regulators (*Il23*) or any downstream effectors (*Lcn2, Cxcl1, S100a9*). Furthermore, histopathological analysis of small intestinal and cecal tissue showed no differences between mice infected with WT *Salmonella* and mice infected with chitinase-deficient strains (Fig. 4 M-N, Fig. S5 A-D). Given the similarity in immune gene expression and the lack of differential pathological scores, we concluded that the phenotypes observed with chitinase-deficient strains were not driven by an altered immune response.

The presence of wild-type chitinases can rescue mutant colonization and invasion.

The chitinases ChiA and STM0233 are predicted to be secreted based on their amino acid sequences [37,38]. We therefore hypothesized that the chitinase-deficient strains would be able to utilize WT chitinases to enhance invasion if they are available during infection. We used the streptomycin-pretreatment mouse model to explore the invasive capabilities of the *Salmonella* strain lacking both chitinases during co-infection with WT *Salmonella*. After 48 h of co-infection, there was no difference in the ability of either strain to invade the colon or ileum (Fig 5A-B). WT *Salmonella* still showed higher colonization in the lumen of the ileum (Fig. 5B). However, the

competitive advantage for WT (2-fold) was drastically reduced compared to the difference in colonization observed during single-infection (39-fold) (Fig 2B). Analyzing organ colonization also did not reveal a competitive advantage for WT *Salmonella* (Fig. 5C). These data demonstrate that the presence of WT *Salmonella* can rescue the invasion and colonization defect of the chitinase-deficient strain during infection. The secretion of chitinases would explain the lack of an invasion defect during co-infection, as the chitinase-deficient strain would still be able to utilize secreted WT chitinases.

Salmonella chitinases induce specific changes to the surface glycome of infected cells.

To examine if *Salmonella* chitinases directly interact with surface glycoproteins of small intestinal epithelial cells during infection, we analyzed the abundance of glycan species during *in vitro* infection with WT *Salmonella* and the chitinase-deficient strains. Infection was performed at an MOI of 1000 to ensure that any glycomic changes would be detectable. We simultaneously performed an invasion assay to confirm that the chitinase-deficient strains also demonstrated the previously observed invasion defect at this higher MOI (Fig. S6). Fig. 6A shows a common *N*-linked glycan species and its saccharide components. Principal component analysis (PCA) revealed distinct groupings for the glycome of uninfected, WT infected, and the chitinase-deficient strain infected cells, indicating that *Salmonella* chitinases induce specific glycomic changes during infection (Fig. 6B). Closer inspection of the changes in the relative abundance of glycans revealed an increase in the abundance of specific glycans when epithelial cells were challenged with the chitinase-deficient strains compared to WT infection. These included various glycans containing GlcNAc, LacNAc, or NeuAc-LacNAc as terminal residues ($HexNAc_4Hex_3DeoxyHex_1$, $HexNAc_4Hex_5DeoxyHex_1$, $HexNAc_3Hex_3$, $HexNAc_4Hex_4$, $HexNAc_3Hex_4NeuAc_1$, $HexNAc_5Hex_5NeuAc_2$) (Fig. 6C). We therefore hypothesized that *Salmonella* chitinases might indeed cleave GlcNAc-containing residues on these glycans. However, other GlcNAc-containing

glycans were unchanged in relative abundance when chitinases were deleted (Table S4, [39]: GPST000225). *Salmonella* chitinases may therefore be interacting with specific glycan species instead of broadly interacting with all GlcNAc-containing glycans. Surprisingly, ChiA and STM0233 seem to share similar activity towards specific glycan residues, as there are only minor differences in the abundances of individual glycans during infection with the single-deletion strains (Fig. 6C, Table S4, [39]: GPST000225).

Interestingly, we also found multiple glycans that increased in abundance upon infection with WT *Salmonella*, but not during infection with the chitinase-deficient strains (Fig. 6D-E). Many of these are high molecular-weight complex or hybrid glycans ($HexNAc_5Hex_3DeoxyHex_1$, $HexNAc_4Hex_6DeoxyHex_1NeuAc_1$, $HexNAc_5Hex_6NeuAc_4$, $HexNAc_5Hex_6DeoxyHex_1$, $HexNAc_3Hex_6DeoxyHex_1$, $HexNAc_5Hex_8DeoxyHex_1$, $HexNAc_5Hex_6DeoxyHex_1NeuAc_2$, $HexNAc_5Hex_6DeoxyHex_1NeuAc_3$) (Fig. 6D), including many glycans that contain Lewis X structures ($HexNAc_5Hex_5DeoxyHex_1NeuAc_1$, $HexNAc_5Hex_7DeoxyHex_1$, $HexNAc_6Hex_6DeoxyHex_1$, $HexNAc_6Hex_7DeoxyHex_1$, $HexNAc_6Hex_7DeoxyHex_1NeuAc_2$) (Fig. 6E-F). The upregulation of these glycans during WT *Salmonella* infection indicates a modulation of the expression of glycans by host cells. Since these changes do not occur during infection with chitinase-deficient strains, the detection of *Salmonella* chitinases or their enzymatic activity by host cells may drive these glycomic changes. Overall, this data suggests that *Salmonella* chitinases modulate the surface glycome during infection via direct enzymatic activity or indirect induction of host cell glycan expression to enhance adhesion and invasion of intestinal epithelial cells (Fig. 7).

Discussion

Bacterial chitinases have recently been recognized as virulence factors for various pathogenic species [40]. However, studies of *Salmonella* chitinases have been mostly limited to the enzymatic activity of ChiA, which was found to cleave chitin, LacNAc, and LacdiNAc molecules [22,23]. A functional role for *Salmonella* chitinases during infection had been suggested based on the observations that *chiA* is upregulated during the infection of epithelial cells, murine macrophages, and the chicken gastrointestinal system [19–21]. One study therefore investigated ChiA's role for host cell invasion and pathogenicity [41]. Deletion of ChiA resulted in only slightly reduced invasion of non-intestinal epithelial cells and no competitive advantage of wild type *Salmonella* over ChiA-deficient *Salmonella* in a mixed infection mouse model, questioning the relevance of *Salmonella* chitinases for pathogenicity. Our study corroborates these results, as we also show that the role of chitinases is cell-type specific and not apparent in mixed infections. However, using different experimental conditions, we were able to elucidate a role for *Salmonella* chitinases during infection.

One role that has been identified for chitinases in other pathogens is the facilitation of binding to intestinal epithelial cells. ChiA of AIEC is known to enhance the adhesion to intestinal epithelial cells [16]. Chitin-binding proteins of *Serratia marcescens* (Cbp21) and *Vibrio cholera* (GbpA) have also been shown to promote adherence to intestinal epithelial cells [17,42]. Here, we demonstrate that both *Salmonella* chitinases are involved in adhesion to intestinal epithelial cells (Fig 1 D-E). This role in adhesion likely explains the invasion defect of the chitinase-deficient strains (Fig 1B-C, 2C), as adhesion is a prerequisite of *Salmonella* invasion [30]. Interestingly, *Salmonella* chitinases may play a greater role in the adhesion to small intestinal tissue than colonic tissue, based on the larger adhesion/invasion defect *in vitro* and the lack of a colonic invasion defect *in vivo* (Fig. 1B-E, 2D). Previous literature has indicated that the binding of *Salmonella* to a variety of epithelial cell lines is mediated by fimbriae specific to each cell type [43]. This suggests a potential role for chitinases as mediators for the binding of fimbriae specific to the small intestines,

such as Pef [44]. Prior to this study, STM0233 has not been studied experimentally. Our data suggest that STM0233 may play a more significant role in adhesion and invasion than ChiA (Fig. 1B-E).

Based on the function of chitinases from other bacterial pathogens, there are a variety of possible explanations as to why *Salmonella* chitinases enhance adhesion. For one, chitinases could be degrading mucins to provide access to the epithelial layer. *Legionella pneumophila* produces a chitinase (ChiA), which is not homologous to *Salmonella* ChiA, that degrades mucins present in the lungs to enhance colonization [10,11]. It is now known that the binding of GbpA of *Vibrio cholerae* to intestinal mucins is responsible for enhanced adhesion to epithelial cells [15]. While interactions with intestinal mucins could potentially contribute to the *in vivo* colonization and invasion defect (Fig. 2C), it does not explain our *in vitro* results (Fig. 1C, E) as the IPEC-1 cell line is not known to be a mucin-producing cell line [45]. Therefore, we focused our study on the *N*-linked glycans present on IPEC-1 cells and did not explore possible interactions with the *O*-linked glycosylation of mucins.

One possible role for chitinases is the liberation of nutritional resources from intestinal glycans to enhance luminal colonization. *Vibrio cholerae* produces a chitinase (ChiA2) that can degrade mucins, releasing saccharides that can be used as a carbon source [14]. Members of the commensal microbiota can also use intestinal glycans as a source of nutrients by producing various types of glycosyl hydrolases [46,47]. *Salmonella* could be using glycans as a nutrient source. However, this seems unlikely since the invasion assays were performed in rich media (Fig 1 B-D), where *Salmonella* would not require an alternative carbon source to replicate efficiently.

Some bacterial chitinases are known to interact with the host immune system to promote infection. For example, one chitinase produced by *Listeria monocytogenes* (ChiA) was found to down-regulate *nos2* expression during murine infection [12]. *L. monocytogenes* strains lacking ChiA

showed decreased colonization of the spleen and liver during murine infection [12,13]. This observation indicated an extraintestinal role for *L. monocytogenes* chitinases in modulating inflammation. In our mouse model of *Salmonella* infection, we detected a minor increase in *Il17* expression in chitinase-deficient strain infected mice, but no changes in the expression of *nos2* or other innate immune genes (Fig. 4A-L). Even though chitinase-deficient strains displayed a colonization defect for the spleen and liver with an intestinal infection model (Fig 3A), there was no colonization defect when *Salmonella* was delivered directly to the peritoneal cavity (Fig. 3B). With this consideration, *Salmonella* chitinases are likely specifically required for small intestinal infection through a mechanism that does not involve innate immune modulation.

Another possible mechanism for enhanced adhesion is through interactions between bacterial chitinases and the host protein Chitinase 3 like 1 (CH3L1). CH3L1 is a chitin-binding protein expressed by various cell types, such as intestinal epithelial cells [18] and macrophages [48], and is associated with inflammatory bowel disease [49,50]. Both CBP21 of *Serratia marcescens* and ChiA of AIEC exploit intestinal CH3L1 expression to adhere to epithelial cells [16,17]. CH3L1 appears to play a role in *Salmonella* infection, as the expression of CH3L1 by colonic epithelial cells was found to enhance *Salmonella* adhesion and invasion [18]. Our study has not explored the possibility that *Salmonella* chitinases promote adhesion by interacting with CH3L1 in a similar manner as CBP21 and ChiA of AIEC.

A likely target for bacterial chitinases are the *N*-linked surface glycoproteins expressed by host cells. *Salmonella* is already known to trigger the removal of sialic acid during infection of colonic cells, which is likely to be mediated by sialidases expressed by *Salmonella* [26,51]. Several other glycosyl hydrolases expressed by *Salmonella* have also been implicated in the modulation of specific glycan species [25]. Importantly, the glycomic changes induced by *Salmonella* infection were not dependent on invasion [26]. Even though ChiA has demonstrated activity towards LacNAc residues [22,23], we did not detect broad removal of LacNAc residues during infection

(Table S4, [39]: GPST000225). Instead, we saw the abundance of specific GlcNAc-containing glycans increase during infection with the chitinase-deficient strains (Fig. 6C). This pattern indicates that chitinases expressed by WT *Salmonella* remove these residues, while other GlcNAc-containing glycans are unaffected. Chitinases may only be required for the removal of GlcNAc residues on specific glycoproteins to facilitate invasion. This hypothesis is supported by previous observations that the type 1 fimbria, FimH, promotes *Salmonella* adhesion and invasion of M cells by specifically binding mannose-containing *N*-linked glycans of surface Glycoprotein 2 (GP2) [52,53]. It has also been shown that the binding of AIEC ChiA to CH3L1 is specifically dependent on the N-glycosylation of CH3L1 [16]. So chitinases may not be required to have broad activity towards all GLcNAc residues. Instead, they could specifically target glycan species that would markedly contribute to invasion.

Furthermore, our data also indicates that host cells are potentially detecting the activity of *Salmonella* chitinases and are modulating their glycome to compensate. We observed an increase in high molecular-weight complex glycans during infection with WT *Salmonella*, potentially driven by host cell regulation (Fig. 6C). Specifically, there was an increase in additional fucose subunits on terminal LacNAc residues forming Lewis X structures (Fig. 6D). Increased fucosylation has been observed in a previous glycomic analysis of *Salmonella* infection, which also identified increased expression of the host cell fucosyltransferases that would be responsible for this fucosylation [25]. It seems that this upregulation of fucosylation is dependent on *Salmonella* chitinase activity, as the relative abundance of Lewis X-containing glycans during chitinase-deficient strain infection is comparable to uninfected cells (Fig. 6E-F). It is important to note that *Salmonella* expresses a fimbrial adhesin, Pef*,* that binds Lewis X structures and is specifically required for small intestinal adhesion [44,54]. *Salmonella* may therefore exploit this upregulation of Lewis X structures as an alternative binding site, which would explain the tissue tropism of chitinase-mediated invasion of the small intestines (Fig. 2C).

Here we elucidated novel roles for *Salmonella* chitinases (ChiA and STM0233) in promoting infection by enhancing small intestinal invasion. We have demonstrated that chitinases promote the adhesion to epithelial cells, which likely drives the enhanced invasion. We also showed that chitinases are required for optimal early small intestinal infection and promote increased dissemination of *Salmonella* into systemic circulation. Increased invasion is linked to modulations of the epithelial cell glycome induced by *Salmonella* chitinases. Chitinases cause alterations in the abundance of specific GlcNAc-containing glycans that would indicate chitinase-mediated cleavage and increase the abundance of Lewis X-containing glycans, likely by stimulating host cell expression.

Materials and Methods

Bacterial Strains

All strains were grown while shaking at 200 rpm in 5 mL of Luria-Bertani (LB) broth (BD Diagnostic Systems) for 16 h at 37 ℃ unless otherwise stated (Table S1).

Table S1- Bacterial strains and plasmids used

Designation	Genotype	Source or Reference
***Salmonella enterica* serovar Typhimurium strains**		
IR715	ATCC 14028, spontaneous Nal^R derivative	[55]
BL212	IR715 Δ*invA*::Cm	This study
BL114	IR715 Δ*STM0233*::Cm	This study
BL122	IR715 Δ*chiA*::Kan	This study

BL130	IR715 Δ*STM0233::*Cm, Δ*chiA::*Kan	This study
BL2	IR715 +pHP45Ω	Vladimir E. Diaz-Ochoa
BL118	IR715 Δ*STM0233::*Cm +pHP45Ω	This study
BL229	IR715 Δ*chiA::*Kan +pHP45Ω	This study
BL168	IR715 Δ*STM0233::*Cm, Δ*chiA::*Kan +pHP45Ω	This study
BL298	IR715 Δ*STM0233::*Cm, *glmS::STM0233* (-344 to +1783)	This study
BL300	IR715 Δ*STM0233::*Cm, Δ*chiA::*Kan, *glmS::STM0233* (-344 to +1783)	This study
BL302	IR715 Δ*STM0233::*Cm, Δ*chiA::*Kan, *glmS::chiA* (-350 to +2124)	This study
BL304	IR715 Δ*chiA::*Kan, *glmS::chiA* (-350 to +2124)	This study
***Escherichia coli* strains**		
S17-1 λpir	*recA thi pro hsdR*$^-$ *M*$^+$ RP4::2-Tc::Mu::Km Tn7 Tp^r Sm^r λpir	[56]
One Shot TOP10 Electrocompetent cells	F- *mcr*A Δ(*mrr-hsd*RMS-*mcr*BC) φ80*lac*ZΔM15 Δ*lac*X74 *rec*A1 *ara*D139 Δ(*ara-leu*)7697 *gal*U *gal*K *rps*L (Str^R) *end*A1 *nup*G λ-	Invitrogen
Bacteriophages		

P22 *HT105/1 int-201*	*HT105/1 int-201*	[57]
P22 H5		[58]
Plasmids		
pGP704	$Carb^R$, ori/R6K, mob/RP4. Suicide vector for homologous recombination	[59]
pHP45Ω	$Strep^R$, $Carb^R$	[60]
pKD3	Cm^R, $Carb^R$, ori/R6K	[61]
pKD4	Kan^R, $Carb^R$, ori/R6K	[61]
pGP704-STM0233::Cm	Cm^R, $Carb^R$, ori/R6K, mob/RP4. Suicide vector containing the deletion construct for homologous recombination	This study
pGP704-*chiA*::Kan	Cm^R, $Carb^R$, ori/R6K, mob/RP4. Suicide vector containing the deletion construct for homologous recombination	This study
pGP704-*invA*::Cm	Kan^R, $Carb^R$, ori/R6K, mob/RP4. Suicide vector containing the deletion construct for homologous recombination	This study

pGRG36	*araC,* P_{BAD}, tnsABCD, rrnD, *bla* ($Carb^R$), *oriT,* pSC101 *ori*^{ts}. Temperature-sensitive plasmid expressing Tn7 transposon machinery.	Nancy Craig (Addgene plasmid #16666; http://n2t.net/addgene:16666; RRID:Addgene_16666) [62]
pGRG36-STM0233	*araC,* P_{BAD}, tnsABCD, rrnD, *bla* ($Carb^R$), *oriT,* pSC101 *ori*^{ts}*, STM0233.* Temperature-sensitive plasmid expressing Tn7 transposon machinery and STM0233.	This study
pGRG36--chiA	*araC,* P_{BAD}, tnsABCD, rrnD, *bla* ($Carb^R$), *oriT,* pSC101 *ori*^{ts}*, chiA.* Temperature sensitive plasmid expressing Tn7 transposon machinery and chiA.	This study
pCR-BluntII-TOPO	P_{lac}, lacZ-α/ccdB, Kan^R, $Zeocin^R$, pUC ori. Vector for subcloning	Invitrogen

410

411 **Mutant Generation**

412 Wild-type *Salmonella* IR715 was used to generate all deletion strains. Deletion constructs
413 containing an antibiotic resistance cassette flanked by sequences homologous to 1kb upstream
414 and downstream of the target gene on a pGP704 suicide vector backbone were generated by
415 Gibson assembly (Table S1). Q5 High-Fidelity DNA Polymerase (New England Biolabs) was used
416 for all cloning PCR reactions. The genome of IR715 was used to generate the homologous

flanking regions for each gene. The primers used to generate the flanking regions of *chiA* were chiA_FR1_fwd, chiA_FR1_rev, chiA_FR2_fwd#2, and chiA_FR2_rev#2. The flanking region for *STM0233* was generated with the primers STM0233_FR1_fwd, STM0233_FR1_rev, STM0233_FR2_fwd, and STM0233_FR2_rev. The flanking region for *invA* was generated with the primers invA-LB_FW, invA-LB_RV, invA-RB_FW, and invA-RB_RV. The *STM0233* and *invA* deletion constructs contained a chloramphenicol resistance cassette, while the *chiA* deletion construct contained a kanamycin resistance cassette. The chloramphenicol resistance cassette was generated by PCR using pKD3 as a template and primers CmR_fwd and CmR_rev for the *STM0223* deletion construct and invA-CmR_FW and invA-CmR_RV for the *invA* deletion construct. The kanamycin resistance cassette was generated by PCR using pKD4 as the template and the primers chiA_KanR_fwd and chiA_KanR_rev#2. pGP704 was digested with the restriction enzymes SalI and EcoRV. The two flanking regions, the antibiotic resistance cassette and the vector backbone, were ligated together using the Gibson Assembly Master Mix (NEBuilder), generating the plasmids pGP704-*STM0233*::Cm, pGP704-*chiA*:Kan, and pGP704-*invA*::Cm. *Escherichia coli* S17 λpir cells were transformed with either pGP704-*STM0233*::Cm, pGP704-*chiA*::Kan, or pGP704-*invA*::Cm and selected for on LB agar with carbenicillin (0.1 mg/mL). The transformation was done by electroporation (Gene Pulser II, Biorad) using 1 µL of a 1:3 dilution of the assembly reaction (in ultrapure H_2O). Single colonies of the resulting *E. coli* S17 λpir cells containing either pGP704-*STM0233*::Cm, pGP704-*chiA*::Kan, or pGP704-*invA*::Cm were grown in LB broth with carbenicillin (0.1 mg/mL). These *E. coli* cultures were plated on LB agar with a culture of IR715 at a 1:1 ratio for conjugation. Plates were incubated at 37 ℃ for 16 h, allowing deletion constructs to be transferred to IR715 and the target genes to be replaced with the antibiotic resistance cassette by homologous recombination. The bacterial lawns were harvested, and the resulting deletion strains, *ΔSTM0233* and *ΔinvA,* were selected for on LB agar with nalidixic acid (0.05 mg/mL) and chloramphenicol (0.03 mg/mL). The *ΔchiA* strain was selected for

on LB agar with nalidixic acid (0.05 mg/mL) and kanamycin (0.1 mg/mL). Two PCR reactions were used to confirm the antibiotic resistance cassettes inserted into the correct location. The primer sets used for these reactions were C2 and STM0233_FR1_out_Fw, and C1 and STM0233_FR2_out_Rv for Δ*STM0233*. The primer sets used for Δ*chiA* were chiA_out_Fw and K1_(Kan_Rv), and chiA_out_Rv and K3_(Kan_Fw). The primer sets used for Δ*invA* were invA_LB_chk_FW and C3, and C1 and invA_RB_chk_RV. The chitinase deletion strains were further examined to confirm that the target genes were deleted. The presence of *STM0233* was detected with the primer pair STM0233_pres_Fw and STM0233_pres_Rv, and *chiA* was detected with the primer pair chiA_pres_Fw and chiA_pres_Rv (Table S2).

Table S2- Primers used for cloning

Primer	**Sequence**
chiA_FR1_fwd	5'-AAAGTGCCACCTGCAGATCTGCAGGCGTAGGCTTCAGCGTGGG-3'
chiA_FR1_rev	5'-CCGGTTCGCTTGCTTTCAAATTTCCTTTTACGTTTCAAAATTGTCG-3'
chiA_KanR_fwd	5'-AGGAAATTTGAAAGCAAGCGAACCGGAATTG-3'
chiA_KanR_rev#2	5'- ATGAAGCCCAATAGAGTCCCGCTCAGAAGAAC-3'
chiA_FR2_fwd#2	5'- CTGAGCGGGACTCTATTGGGCTTCATGATTCAAGCCCCGGTTTAC-3'
chiA_FR2_rev#2	5'- GATCGAATTCCCGGGAGAGCTCGATCGCCGGGTTTCGCCGGCA -3'
STM0233_FR1_fwd	5'-AAAGTGCCACCTGCAGATCTGCAGGCGTAGAACTGACGCGCAAAATC-3
STM0233_FR1_rev	5'-TCCGTCACAGGTAAATTTTCTCCTTGAAGGGTAGTTC-3'
CmR_fwd	5'-CAAGGAGAAAATTTACCTGTGACGGAAGATCACTTCGCAG-3'

CmR_rev	5'-AGGATTTATCTTACTTACGCCCCGCCCTGCC-3'
STM0233_FR2_fwd	5'-GGCGGGGCGTAAGTAAGATAAATCCTGTCGGTG-3'
STM0233_FR2_rev	5'-GATCGAATTCCCGGGAGAGCTCGATCGTAAGTCGAATTGGTGATAAC-3'
invA-LB_FW	5'-AAAGTGCCACCTGCAGATCTGCAGGACGGCCTCGTTCACCGATAAG-3'
invA-LB_RV	5'-TCCGTCACAGGTAGGGCTTAATTAAGGAAAAGATCTATGCAAC-3'
invA-CmR_FW	5'-CTTAATTAAGCCCTACCTGTGACGGAAGATCACTTCGCAG-3'
invA-CmR_RV	5'-CAGGATACCTATACTTACGCCCCGCCCTGCC-3'
invA-RB_FW	5'-GGCGGGGCGTAAGTATAGGTATCCTGTTAATATTAAATTAAG-3'
invA-RB_RV	5'-GATCGAATTCCCGGGAGAGCTCGATACAAAAATTTGTCCAGTCG-3'
C2	5'-GATCTTCCGTCACAGGTAGG-3'
STM0233_FR1_out_FW	5'-AGGTGGAACTGGAGTTTG-3'
C1	5'-TTATACGCAAGGCGACAAGG-3'
STM0233_FR2_out_Rv	5'-GAAATGGGTATAGGGTACCC-3'
STM0233_pres_Fw	5'-CCCTGGCTACTATGTTTGC-3'
STM0233_pres_Rv	5'-GGTAGCTGGTGGTCTTATC-3'
chiA_out_Fw	5'-GAGATGACGTCAAAACCTGGT-3'
K1_(Kan_Rv)	5'-CAGTCATAGCCGAATAGCCT-3'

chiA_out_Rv	5'-GGCGCGATTTGCATCTCATC-3'
K3_(Kan_Fw)	5'-CTCGTGCTTTACGGTATC-3'
chiA_pres_Fw	5'-AGGCAATATGTCCCAACCGG-3'
chiA_pres_Rv	5'-CGCCGTTGTCCTGATCGATA-3'
invA_LB_chk_FW	5'-CCACTTACTTCCAGTGCGG-3'
invA_RB_chk_Rv	5'-CAGAACAGCGTCGTACTATTG-3
STM0233_Tn7Com_FW	5'-CCCGGGTCGATTCCATCATTCCGGAG-3'
STM0233_Tn7Com_RV	5'-CTCGAGATGCAAAGCACCGACAGGAT-3'
chiA_Tn7Com_FW	5'-CCCGGGTCCTGGTTGTCTGTGGTGAC-3'
chiA_Tn7Com_RV	5'-CTCGAGATGAAGCCCAATACATCGGC-3'
Tn7_ck_FW	5'-GCCAGGGCCTTAAAGAAGAG-3'
Tn7_ck_RV	5'-GCCGCGTAACCTGGCGAAAT-3'

452

453 The *Salmonella* IR715 Δ*STM0233 ΔchiA* strain was generated by transduction using the P22
454 *HT105/1 int-201* bacteriophage (Table S1). A culture of the IR715 Δ*chiA* strain was infected with
455 P22 *HT105/1 int-201* for 8 h at 37 ℃. The phage was isolated by the centrifugation of the infected
456 culture, and chloroform was added to the collected supernatant. Bacteriophage transduction was
457 performed by plating 200 µL of a 16 h IR715 Δ*STM0233* culture and 1-20 µL of the isolated P22
458 phage onto LB agar with kanamycin (0.1 mg/mL). Plates were incubated at 37 ℃ overnight, and

459 the resulting colonies of transductants were cross-streaked against the P22 H5 phage on Evans
460 blue-Uranine (EBU) agar to isolate phage-free true lysogens.

461 Complementation of the chitinase deletion strains was done by transposon-mediated insertion of
462 the full chitinase gene and endogenous promoter into the Tn7 locus [62]. Chitinase genes and
463 their endogenous promoters were amplified using Q5 High-Fidelity DNA Polymerase (New
464 England Biolabs) with wild-type *Salmonella* IR715 as the template and the primer sets
465 STM0233_Tn7Com_FW and STM0233_Tn7Com_RV or chiA_Tn7Com_FW and
466 chiA_Tn7Com_RV, which carry restriction sites for either XmaI or XhoI on their 5' end. The gene
467 fragments were sub-cloned into Zero Blunt TOPO PCR vector (Invitrogen) and electroporated into
468 One Shot Top10 cells (Invitrogen). The plasmid containing the cloned chitinase gene was isolated
469 using the Qiaprep spin miniprep kit (Qiagen). Restriction digestion of the plasmid was done with
470 XhoI and XmaI, and the chitinase gene fragment was isolated via gel extraction with the QIAQuick
471 Gel Extraction kit (Qiagen). pGRG36 was also digested with XhoI and XmaI and extracted via gel
472 extraction using the QIAEX II gel extraction kit (Qiagen). The digested pGRG36 and cloned
473 chitinase gene were ligated together using ElectroLigase (New England Biolabs) and used to
474 transform One Shot Electrocompetent cells. Transformants were selected for by growing at 32 ℃
475 on LB agar with carbenicillin (0.1 mg/mL). pGRG36-*STM0233* and pGRG36-*chiA* were isolated
476 using the Plasmid Midi kit (Qiagen), and Sanger sequencing was performed to confirm that the
477 cloned chitinase genes had the correct sequence. Sanger sequencing was performed by the
478 Genome Research core at the University of Illinois Chicago. The chitinase deletion strains
479 (BL114, BL122, and BL130) were transformed with pGRG36-*STM0233* or pGRG36-*chiA*.
480 Transformants were isolated and grown in an LB culture at 32 ℃ overnight. Overnight cultures
481 were serially diluted in PBS and plated for single colonies on LB agar plates. Plates were
482 incubated at 42 ℃ overnight to block plasmid replication (pGRG36 has a temperature-sensitive
483 origin of replication). Single colonies were streaked on LB agar and incubated at 42 ℃ overnight

to ensure plasmid loss. Insertion of the chitinase genes in the Tn7 locus was confirmed by colony PCR. The presence of *STM0233* was detected with the primer pair STM0233_pres_Fw and STM0233_pres_Rv, and *chiA* was detected with the primer pair chiA_pres_Fw and chiA_pres_Rv. A primer set that flanks the Tn7 insertion site (Tn7_ck_FW and Tn7_ck_RV) was used to confirm the insertion site.

Tissue Culture

The T84 colonic epithelial cell line (ATCC Cat# CCL-248; RRID:CVCL_0555) and IPEC-1 small intestinal epithelial cell line (DSMZ Cat# ACC-705, RRID:CVCL_2245) were grown in T75 flasks using 20 mL DMEM/F12 + 10% FBS + 1x antibiotic/antimycotic (Gibco). Cultures were incubated at 37 ℃ with 5% CO_2. Media was replaced every other day. Cell cultures were split with 0.25% trypsin + EDTA (Gibco) when cells reached 80% confluency.

Invasion assay

T84 or IPEC-1 cells were seeded onto a 24-well plate at a density of $5x10^5$ cells/well with media lacking antibiotics/antimycotics and incubated overnight at 37 ℃. *Salmonella* strains were grown for 16 h in liquid LB without shaking at 37 ℃. Bacterial cell number was quantified by measuring the OD_{600} of the cultures. $1x10^9$ cells of each strain were centrifuged, resuspended in DMEM/F12, and serially diluted. Epithelial cells were infected with $5x10^5$ cells of *Salmonella* (multiplicity of infection (MOI) =1). Infected cells were incubated at 37 ℃ for 1 h. The inoculum was serially diluted and plated on LB agar to confirm bacterial numbers. After infection, the media was removed via vacuum, and wells were washed 3 times with 500 µL phosphate-buffered saline (PBS). 500 µL of DMEM/F12 + 10% FBS + 0.1 mg/mL gentamicin was added to the wells and incubated at 37 ℃ for 1 h to kill extracellular bacteria. After incubation, the wells were washed with PBS and lysed by incubation with 1% Triton X-100 for 5 mins. Cells were disrupted and harvested by scraping wells and pipetting, were serially diluted, and plated on LB agar to quantify

508 bacterial cells that invaded. The percentage of cells recovered relative to the inoculum was
509 calculated.

510 **Adhesion Assay**

511 This assay was adapted from a previous study [63]. T84 cells were seeded onto a 24-well plate
512 at a density of $2x10^6$ cells/well to achieve confluency and prevent nonspecific binding of
513 *Salmonella* to the bottom of the well. IPEC-1 cells were seeded at a density of $5x10^5$ cells/well,
514 which was sufficient to achieve confluency. The media used lacked antibiotics/antimycotics, and
515 the cells were incubated overnight at 37 ℃. *Salmonella* strains were grown in liquid LB without
516 shaking for 16 h at 37 ℃. T84 and IPEC-1 cells were incubated in DMEM/F12 + 10% FBS + 2
517 µg/ml Cytochalasin D (Sigma-Aldrich) at 37 ℃ for 1 h to block actin-dependent invasion. The
518 OD_{600} was measured for each *Salmonella* culture, and $1x10^9$ cells of each strain were centrifuged,
519 resuspended in DMEM/F12, and serially diluted. While in the presence of Cytochalasin D,
520 epithelial cells were infected at a MOI=1. Infection was carried out for 30 minutes, and epithelial
521 cells were washed 4 times with PBS and lysed with 1 mL 1% Triton X-100. Cells were disrupted
522 and harvested by scraping wells and pipetting, serially diluted, and plated on LB agar to quantify
523 adherent bacterial cells. The percentage of cells recovered relative to the inoculum was
524 calculated.

525 ***In vitro* Growth Curve**

526 Colloidal chitin was made based on a previous study [64]. Crab shell flakes were ground by mortar
527 and pestle and sieved through a 130 mm two-piece polypropylene Büchner filter. 20 g of sieved
528 crab shell flakes were placed in a beaker, and 150 mL of 12 M HCl was added slowly with
529 continuous stirring. The chitin-HCl mixture was stirred every 5 min over the course of an hour.
530 The mixture was then passed through 8 layers of cheesecloth to remove large chunks into a 2 L
531 plastic beaker. 2 L of ice-cold MilliQ water was added and incubated at 4 ℃ for 16 h. After

532 incubation, 3 L of tap water was passed through the colloidal chitin cake on two layers of coffee
533 filter paper in a Büchner funnel connected to a vacuum filtration flask until the pH of the filtrate
534 was 7.0. Excess moisture was removed by pressing the colloidal chitin cake between coffee filter
535 paper. The colloidal chitin cake was sterilized in an autoclave and used to make M9 + 0.4%
536 colloidal chitin medium (M9 + chitin). The bacterial concentrations of 16 h *Salmonella* cultures
537 grown in LB were determined by measuring OD_{600}. 20 mL of LB or M9 + chitin was inoculated
538 with 1 x 10^5 cells of *Salmonella*. Cultures were incubated shaking at 37 ℃, and samples were
539 taken at indicated time points, serially diluted in PBS, and plated on LB agar.

540 **Mouse Infection**

541 A streptomycin-pretreatment mouse model was used for the *in vivo* infections [33], where each
542 mouse is considered an experimental unit. Single infection experiments were repeated twice with
543 3-5 mice per treatment group. 8 week-old female C57BL/6 mice were purchased from a maximum
544 barrier facility at Jackson Laboratory and were free of *Enterobacteriaceae* (tested by plating fecal
545 samples on MacConkey agar). Mice were housed for 1 week after arrival to allow for their
546 acclimation and given water and food *ad libitum* (mice were fed Teklad Irradiated LM-485 mouse
547 diet 7912). Mice were treated with 100 µL of 200 mg/mL streptomycin (Calbiochem) in water by
548 oral gavage. 24 h after treatment, mice were infected by oral gavage with 100 µL of 1x10^{10}
549 cells/mL of *Salmonella* in LB broth from a 16 h culture. For co-infections, mice were infected with
550 a 1:1 ratio of both *Salmonella* strains. The *Salmonella* strains used carry plasmid pHP45Ω, which
551 confers resistance to streptomycin and carbenicillin. Fecal samples were collected at 8 hpi and
552 24 hpi and either snap-frozen or plated on LB agar + carbenicillin (0.1 mg/mL). At 48 hpi (or 96
553 hpi), mice were euthanized by CO_2 asphyxiation and subsequent cervical dislocation. Immediately
554 after euthanasia, the Peyer's patches, mesenteric lymph nodes, spleen, liver, and luminal
555 samples from the colon and ileum were collected, homogenized, and plating on LB agar with the
556 appropriate antibiotic. Colony-forming units were normalized to the weight of each sample (mg).

Cecum and luminal colon samples were snap-frozen. Ileum and cecum samples were collected and fixed in formalin for histological analysis. Tissue was collected from the terminal ileum and proximal colon, and a gentamicin protection assay was performed. The tissue was incubated in PBS + 0.1 mg/mL gentamicin for 30 mins, washed with PBS, homogenized, and plated on LB agar + carbenicillin (0.1 mg/mL). For co-infection, the mutant strain was quantified by plating on LB agar + chloramphenicol (0.03 mg/mL). WT colonization was calculated by subtracting the mutant CFUs from the CFUs appearing on LB agar + carbenicillin. A competitive index was calculated by dividing CFU/mg of recovered WT by CFU/mg of recovered mutant. This competitive index was corrected based on the ratio of each strain in the inoculum, determined by serial dilution followed by plating on LB agar. Corrected CI= (WT colonization/mutant colonization)/ (WT inoculum/mutant inoculum).

For intraperitoneal infection, 9 week-old female C57BL/6 mice were infected via intraperitoneal injection with 100 µL of $1x10^5$ cells/ml of *Salmonella* in LB broth from a 16 h culture. Mice were sacrificed at 48 hpi, and the spleen and liver were collected. Samples were homogenized and plated on LB agar and the appropriate antibiotic to quantify colonization.

Mouse experiments were performed in accordance with protocols and guidelines approved by the Institutional Animal Care Committee (20-016) of the University of Illinois Chicago.

Histopathology

Tissue sections were fixed with formalin and embedded in paraffin wax. Embedding was done by the Research Histology core at the University of Illinois Chicago. The tissue was then sectioned via microtome and transferred to slides. Before staining, deparaffinization was performed. The tissue slides were immersed in xylene for 10 min, 100% ethanol for 10 min, 90% ethanol for 2 min, 70% ethanol for 2 min, and PBS for 5 min. The tissue slides were then stained with hematoxylin for 30 seconds, washed with tap water, then stained with eosin for 10 min. Slides

were dehydrated by immersion in serial increases of ethanol concentrations (50%-100%), then immersed in xylene. Coverslips were then mounted to the tissue slides and allowed to dry.

Tissue sections were scored for pathology by a board-certified pathologist in a blinded fashion following an approach established by Barthel and colleagues [33] as summarized below.

Submucosal edema was scored as follows: 0 = no pathological changes; 1 = mild edema (submucosa accounts for <50% of the diameter of the entire intestinal wall [tunica muscularis to epithelium]); 2 = moderate edema; the submucosa accounts for 50 to 80% of the diameter of the entire intestinal wall; and 3 = profound edema (the submucosa accounts for >80% of the diameter of the entire intestinal wall).

Polymorphonuclear granulocytes (PMN) in the lamina propria were enumerated in 10 high-power fields (x400 magnification), and the average number of PMN/high-power fields was calculated. The scores were defined as follows: 0 = <5 PMN/high-power field; 1 = 5 to 20 PMN/high-power field; 2 = 21 to 60/high-power field; 3 = 61 to 100/high-power field; and 4 = >100/high-power field. Transmigration of PMN into the intestinal lumen was consistently observed when the number of PMN was >60 PMN/high-power field.

The average number of goblet cells per high-power field (magnification, x400) was determined from 10 different regions of the cecal epithelium. Scoring was as follows: 0 = >28 goblet cells/high-power field (magnification, x400); 1 = 11 to 28 goblet cells/high-power field; 2 = 1 to 10 goblet cells/high-power field; and 3 = <1 goblet cell/high-power field.

Epithelial integrity was scored as follows: 0 = no pathological changes detectable in 10 high-power fields (x400 magnification); 1 = epithelial desquamation; 2 = erosion of the epithelial surface (gaps of 1 to 10 epithelial cells/lesion); and 3 = epithelial ulceration (gaps of >10 epithelial cells/lesion).

Two independent scores for submucosal edema, PMN infiltration, goblet cells, and epithelial integrity were averaged for each tissue sample. The combined pathological score for each tissue

sample was determined as the sum of these averaged scores. It ranges between 0 and 13 arbitrary units and covers the following levels of inflammation: 0 intestine intact without any signs of inflammation; 1 to 2 minimal signs of inflammation ; 3 to 4 slight inflammation; 5 to 8 moderate inflammation; and 9 to 13 profound inflammation.

RNA Extraction

In vivo: Cecum samples collected from mice 48 hpi were homogenized by mortar and pestle and liquid nitrogen. Because mice are treated with streptomycin 24 h prior to infection, we collected cecum samples from uninfected mice 72 h after streptomycin treatment as a control. The homogenate was transferred to 1 mL of Tri-Reagent (Molecular Research Center) for RNA extraction. RNA was extracted with 0.1 mL of bromo-3-chloropropane, centrifuged, and the upper phase was precipitated with 0.5 mL isopropanol. After centrifugation, pellets were washed twice with 1 mL of 75% ethanol in RNase-free water. The RNA pellet was then resuspended in RNase-free water. RNA was treated with DNase using the Turbo DNA-free kit (Invitrogen). For fecal samples, RNA was extracted from snap-frozen luminal colon samples collected during the single infection mouse experiments. RNA extraction was performed using the Qiagen RNeasy PowerMicrobiome kit, and DNase treatment was performed with the Turbo DNA-free kit.

In vitro: A 16 h culture of WT *Salmonella* was sub-cultured (1:100) into LB or DMEM/12 +10% FBS. Cultures were incubated for 3 h at 37 ℃, shaking at 200 rpm. Culture cell concentration was measured by OD_{600}, and $1x10^9$ cells were pelleted by centrifugation. RNA extraction was performed on the pellet using the Invitrogen RiboPure Bacteria kit. RNA extraction was followed by DNase treatment using the Turbo DNA-free kit.

RT-qPCR

Reverse transcription was performed with the High Capacity cDNA Reverse Transcription Kit (Applied Biosystems). For *Salmonella* RNA, reactions were also performed without the addition

of reverse transcriptase to confirm that there was no amplification of DNA in qPCR reactions. 1000 ng of RNA was used for the reverse transcription reaction. The reverse transcription cycle consisted of 10 minutes at 25 ℃ followed by 120 minutes at 37 ℃ and 5 minutes at 85 ℃. qPCR was performed using the Fast SYBR Green Master Mix (Applied Biosystems) on the Viia7 Real-time PCR system at the Genome Research core at the University of Illinois at Chicago. The qPCR reaction cycle consisted of 20 seconds at 95 ℃ followed by 40 cycles of 3 seconds at 95 ℃ and 30 seconds at 60 ℃. Reactions were performed in duplicate. Relative expression was calculated based on the ΔCT values. For the analysis of chitinase expression, the CT value of the house-keeping gene (*gmk*) was subtracted from the CT value of the gene of interest, giving the ΔCT value. Relative expression= $2^{(-\Delta CT)}$. For analysis of murine immune gene expression, the CT value of the housekeeping gene (*actb*) was subtracted from the CT value of the gene of interest, giving the ΔCT value. The ΔCT value of uninfected mice was subtracted from the ΔCT value of infected mice, giving the ΔΔCT value. Relative expression= $2^{(-\Delta\Delta CT)}$ (Table S3).

Table S3- Primers used for RT-qPCR

Primers			
Species	**Target**	**Primer pairs**	**Reference**
Salmonella enterica serovar Typhimurium	*gmk*	5'-TTGGCAGGGAGGCGTTT-3'	[65]
		5'-GCGCGAAGTGCCGTAGTAAT-3'	
Salmonella enterica serovar Typhimurium	*STM0233*	5'-ATCAGGTTTCGGCGTCACTA-3'	This study
		5'-CCGGCACTTTCAGGTAGTTG-3'	

Salmonella enterica serovar Typhimurium	*chiA*	5'-TGATACGCCAGCAGATGACA-3'	This study
		5'-AACGGTAGAAGCATCCCACT-3'	
Mus Musculus	*Actb*	5'-GGCTGTATTCCCCTCCATCG-3'	[66]
		5'-CCAGTTGGTAACAATGCCATGT-3'	
Mus Musculus	*Duox2*	5'-GCACTGTGCAGAACAGCTAGGACAAC-3'	[66]
		5'-ACCTCATCACCTTCTTGCGGGAG-3'	
Mus Musculus	*Cxcl1*	5'-TGCACCCAAACCGAAGTCAT-3'	[66]
		5'-TTGTCAGAAGCCAGCGTTCAC-3'	
Mus Musculus	*IL17a*	5'- GCTCCAGAAGGCCCTCAGA-3'	[66]
		5'-AGCTTTCCCTCCGCATTGA-3'	
Mus Musculus	*Ifng*	5'-TCAAGTGGCATAGATGTGGAAGAA-3'	[66]
		5'-TGGCTCTGCAGGATTTTCATG-3'	
Mus Musculus	*Nos2*	5'-TTGGGTCTTGTTCACTCCACGG-3'	[66]
		5'-CCTCTTTCAGGTCACTTTGGTAGG-3'	
Mus Musculus	*Il22*	5'-GGCCAGCCTTGCAGATAACA-3'	[66]
		5'-GCTGATGTGACAGGAGCTGA-3'	
		5'-GCAACTGTTCCTGAACTCAACT-3'	

Mus Musculus	*Il1b*	5'-ATCTTTTGGGGTCCGTCCAACT-3'	[67]
Mus Musculus	*S100a9*	5'-GGTGGAAGCACAGTTGGCA-3'	[66]
		5'-GTGTCCAGGTCCTCCATGATG-3'	
Mus Musculus	*Il23*	5'-ATGCTGGATTGCAGAGCAGTA-3'	Primer Bank ID: 13752579a1 [68]
		5'-ACGGGGCACATTATTTTTAGTCT-3'	
Mus Musculus	*Tnf*	5'-ATGGCCTCCCTCTCATCAGT-3'	[69]
		5'-CTTGGTGGTTTGCTACGACG-3'	
Mus Musculus	*Il6*	5'-CTGCAAGAGACTTCCATCCAG-3'	Primer Bank ID: 13624310c1 [68]
		5'-AGTGGTATAGACAGGTCTGTTGG-3'	
Mus Musculus	*Lcn2*	5'-ACATTTGTTCCAAGCTCCAGGGC-3'	[66]
		5'-CATGGCGAACTGGTTGTAGTCCG-3'	

643

644 **Glycome analysis**

645 Infection of IPEC-1 cells was carried out similar to the invasion assays at an MOI of 1:1000. After
646 infection, wells were washed twice with PBS, and cells were frozen at -80 ℃. Cells were thawed
647 and washed twice with PBS to remove the lysed cell debris and cytoplasmic proteins. Next, 200
648 µL PBS and 3 µL PNGase F were added to each well and incubated at 37 ℃ for 18 hrs to release
649 surface *N*-glycans. A sealing film (Axygen™ PCRSPS) was employed to cover the well plate to

prevent evaporation. The released *N*-glycans solution was collected, and the well was washed with 200 µL PBS. The wash solution was collected and combined with the previously released *N*-glycan solution, dried, and redissolved in 100 µL water. *N*-glycans were then dialyzed against a 500-1000 MWCO dialysis membrane to remove salts and small molecules. The dialyzed sample was then reduced and permethylated prior to LC-MS/MS analysis, as previously reported [70–72]. Briefly, the dried sample was dissolved in 10 µL borane-ammonia complex solution (10 mg/mL) and incubated in a 60 ℃ water bath for 1h. After reduction, 1 mL of methanol was added to each sample and dried. The methanol addition-dry cycle was repeated 3 times to remove borates. Next, a spin column was packed with sodium hydroxyl beads (suspended in DMSO) and washed twice with 200 µL DMSO. Reduced glycans were resuspended in 30 µL DMSO, 1.2 µL water, and 20 µL iodomethane. The sample was loaded on the column and incubated for 25 min. Then, 20 µL iodomethane was added to each column and incubated for 15 min. After incubation, permethylated glycan solution was collected by centrifuging at 1,800 rpm. The column was then washed with 30 µL acetonitrile (ACN), and the ACN solution was combined with permethylated glycan solution and dried. The reduced and permethylated sample was ready for LC-MS/MS analysis.

Samples were analyzed using an UltiMate 3000 nanoLC system coupled to an LTQ Orbitrap Velos mass spectrometer. The samples were resuspended in 8 µL solution (20% ACN, 80% water, 0.1% formic acid) and injected 6 µL. A PepMap trap column (75 µm* 2 cm, C18, 3 µm, Thermo) was used for online purification. The *N*-glycomic analysis was performed on a PepMap column (75 µm * 15 cm, C18, 2 µm, Thermo) at 55 ℃ at 0.35 µL/min flow rate. A gradient of mobile phase solvents A (98% water with 0.1% FA) and B (98% ACN with 0.1% FA) was used as follows: 0 - 10 min, 20% B; 10 - 11 min, 20% - 42% B; 11 - 48 min, 42% - 55% B; 48 - 49 min, 55% - 90% B; 49 - 54 min, 90% B; 54 - 55 min, 90% - 20% B; 55 - 60 min, 20% B. The MS was performed in positive mode. The full MS scan had a range of 700−2000 *m/z* at a mass resolution of 100,000.

675 The CID (collision-induced dissociation) was used for MS^2 at a normalized collision energy of 35,
676 activation Q of 0.25, and activation time of 10 ms. The data were first processed by MultiGlycan
677 software [73], then manually checked via full MS and MS^2 to remove false positives.

678 **Statistical Analysis**

679 Statistical analysis was performed with Graphpad Prism software v9 (RRID:SCR_002798). Data
680 were tested for normality using the Shapiro-Wilk test and confirmed visually via QQ plot. For data
681 found to follow a lognormal distribution, data were transformed to their natural log values before
682 analysis. Unless otherwise specified, all multiple comparisons analyses compared samples to the
683 WT control. For invasion assays, the percent recovery was analyzed with a one-way ANOVA with
684 Dunnett's multiple comparison test. For adhesion assays, the percent recovery was analyzed with
685 a mixed-effect analysis with Dunnett's multiple comparison test. For mouse single infection
686 experiments, a one-way ANOVA with Dunnett's multiple comparison test (Intragastric) or an
687 unpaired *t*-test was performed (Intraperitoneal). For mouse co-infection experiments, a paired *t*-
688 test was performed with the absolute values and the competitive index was analyzed with a one-
689 sample *t*-test against our null hypothesis that the competitive index equaled one. For *in vitro*
690 chitinase gene expression analysis, an unpaired *t*-test was performed. *In vivo* relative expression
691 of chitinase expression was analyzed with a one-sample *t*-test against our null hypothesis (relative
692 expression=1). For murine gene expression, a one-way ANOVA with Dunnett's multiple
693 comparison test was performed. Analysis of growth curves was done with a mixed-effect analysis
694 and Tukey's multiple comparisons test. For the glycome analysis, the relative abundance for each
695 glycan was calculated by dividing the individual glycan abundance by the total glycan abundance.
696 A Mann-Whitney *U* test was then performed comparing samples to WT or uninfected. The relative
697 abundance of Lewis X structures was calculated by dividing the total number of glycans that
698 contain these structures by the total glycan abundance of each sample. A one-way ANOVA with

699 Dunnett's multiple comparison test was then performed. For all statistical tests, significance was
700 set at $\alpha=0.05$.

701 **Acknowledgements**

702 We thank Clayton Wollner and Kristen Lednovich for technical assistance in initial experiments.
703 We thank Dara Kiani, Amisha Rana, Kelly Perfecto, Kanchan Jaswal, and Olivia Todd for their
704 careful review of this manuscript. The model was created using biorender.com.

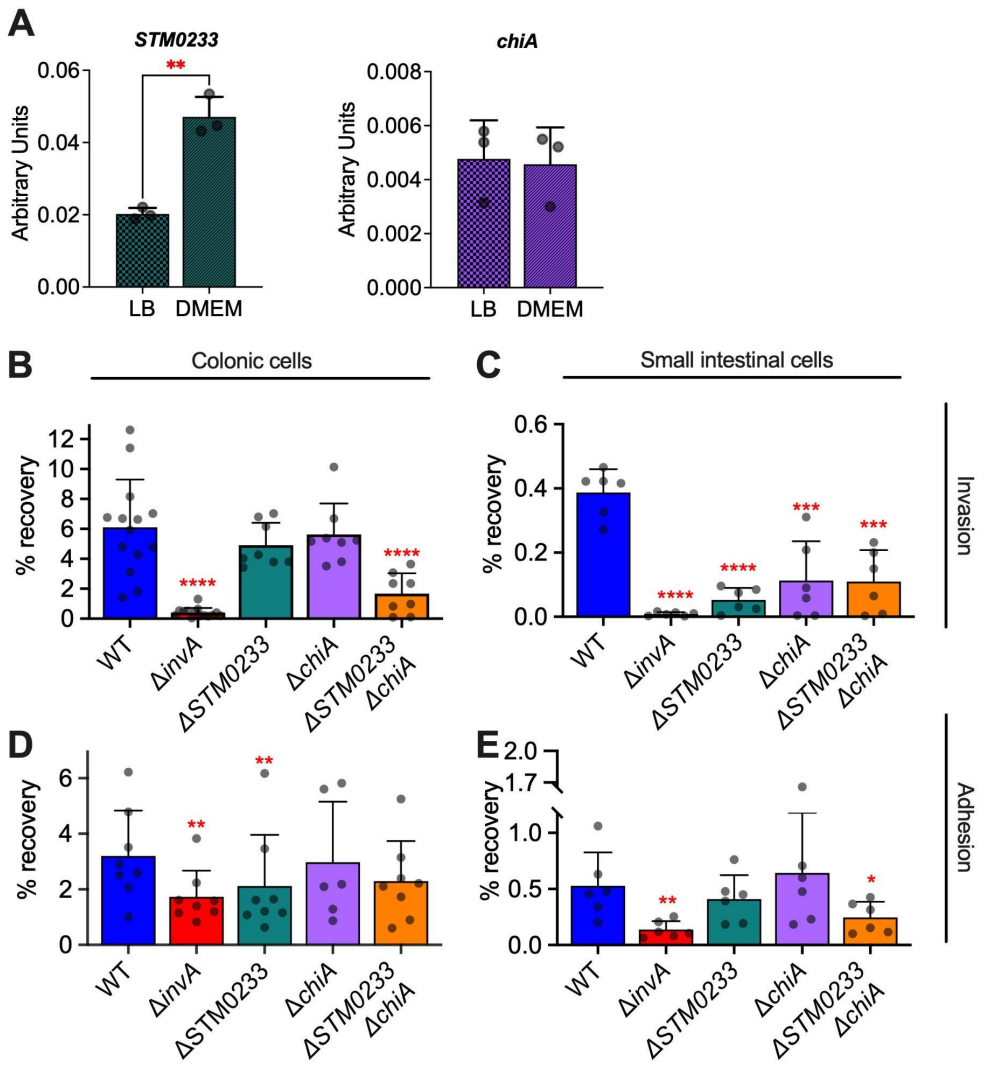

Fig. 1. *Salmonella* chitinases contribute to intestinal epithelial cell adhesion and invasion *in vitro*.

(A) mRNA expression of *Salmonella* chitinases during mid-log phase of growth in LB or DMEM/F12 + 10% FBS measured by RT-qPCR. Expression is normalized to the housekeeping gene *gmk*. n=3. (B) Gentamicin protection assay of *Salmonella* infected (MOI:1) colonic epithelial cells (T84). WT n=14, **Δ***invA* n=14, **Δ***STM0233* n=8, **Δ***chiA* n=8, **Δ***STM0233* **Δ***chiA* n=8. (C) Gentamicin protection assay of *Salmonella* infected (MOI:1) small intestinal epithelial cells (IPEC-1). n=6. (D) Adhesion assay of Cytochalasin D treated (2 µg/mL), *Salmonella* infected (MOI:1)

colonic epithelial cells (T84). WT n=8, **Δ***invA* n=8, **Δ***STM0233* n=8, **Δ***chiA* n=6, **Δ***STM0233* **Δ***chiA* n=8. (E) Adhesion assay of Cytochalasin D treated (2 µg/mL), *Salmonella* infected (MOI:1) small intestinal epithelial cells (IPEC-1). n=6. Bars represent mean ± SD. Statistics: (A) unpaired *t*-test. (B-E) Stars indicate significance compared to the WT control by (B,D) one-way ANOVA with Dunnett's multiple comparison test or (C,E) mixed-effect analysis with Dunnett's multiple comparison test. *=$p<0.05$, **=$p<0.01$.

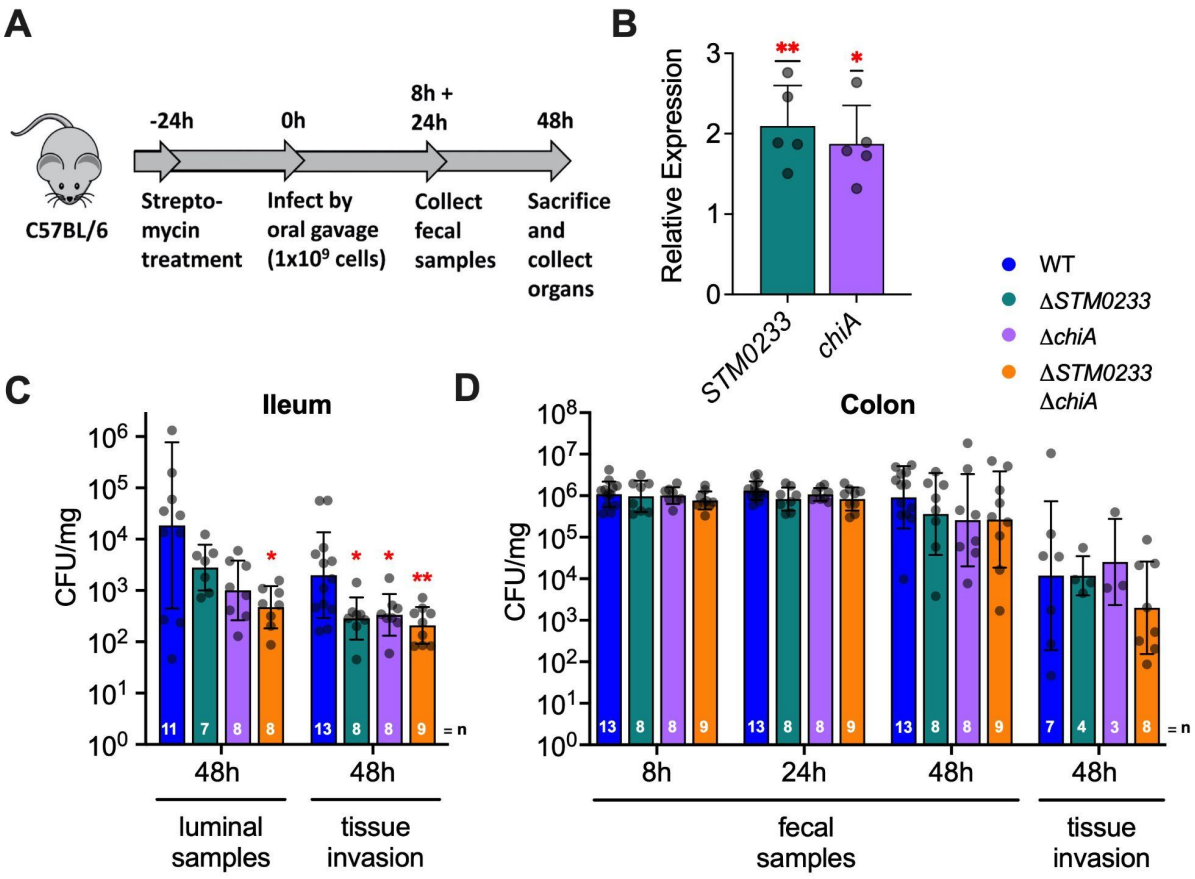

731

732 **Fig. 2. *Salmonella* chitinases are required for the colonization and invasion of small**

733 **intestinal epithelial cells *in vivo*.**

734 (A) Streptomycin pre-treatment mouse model of *Salmonella* infection. (B) mRNA expression of

735 *Salmonella* chitinases extracted from colonic luminal samples collected 48 hpi. Expression is

736 normalized to the housekeeping gene *gmk*. Expression is represented relative to mid-log

737 expression in LB. n= 5. Bars represent mean ± SD. (C) Luminal samples from the terminal ileum

738 were collected 48 hpi to determine *Salmonella* colonization. Invasion was determined with a

739 gentamicin protection assay performed on the terminal ileum. (D) *Salmonella* colonies recovered

740 from fecal samples collected at 8 and 24 hpi. Fecal samples at 48 hpi were collected directly from

741 the lumen of the colon. Invasion of colonic tissue was determined with a gentamicin protection

742 assay. Bars represent geometric mean ± geometric SD. Statistics: (B) one-sample *t*-test against

743 our null hypothesis (relative expression=1) (C-D) Stars indicate significance compared to the WT
744 control by one-way ANOVA with Dunnett's multiple comparison test. *=p<0.05, **=p<0.01.
745
746

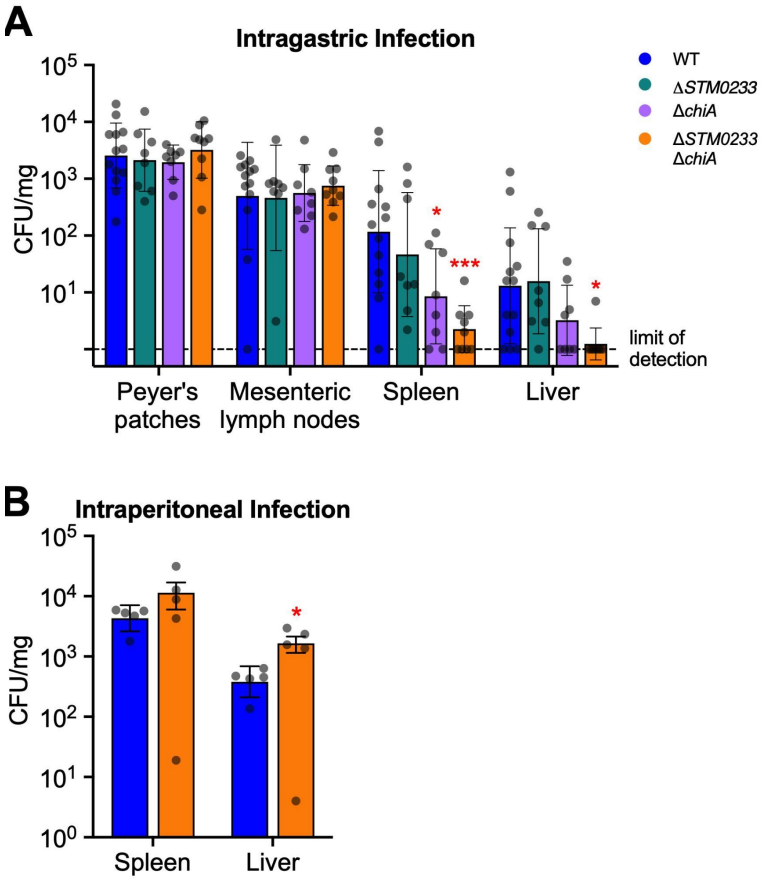

747
748 **Fig. 3. Chitinase-mediated invasion of intestinal tissue contributes to *Salmonella***
749 **dissemination.**
750 (A) Colonization of the Peyer's patches, mesenteric lymph nodes, spleen, and liver 48 h after
751 intragastric infection. WT n=13, **Δ***STM0233* n=8, **Δ***chiA* n=8, **Δ***STM0233* **Δ***chiA* n=9. (B)
752 Colonization of the spleen and liver 48 h after intraperitoneal infection. n= 5. Bars represent
753 geometric mean ± geometric SD. Statistics: Stars indicate significance compared to the WT
754 control by one-way ANOVA with Dunnett's multiple comparison test. *=p<0.05, ***=p<0.001.

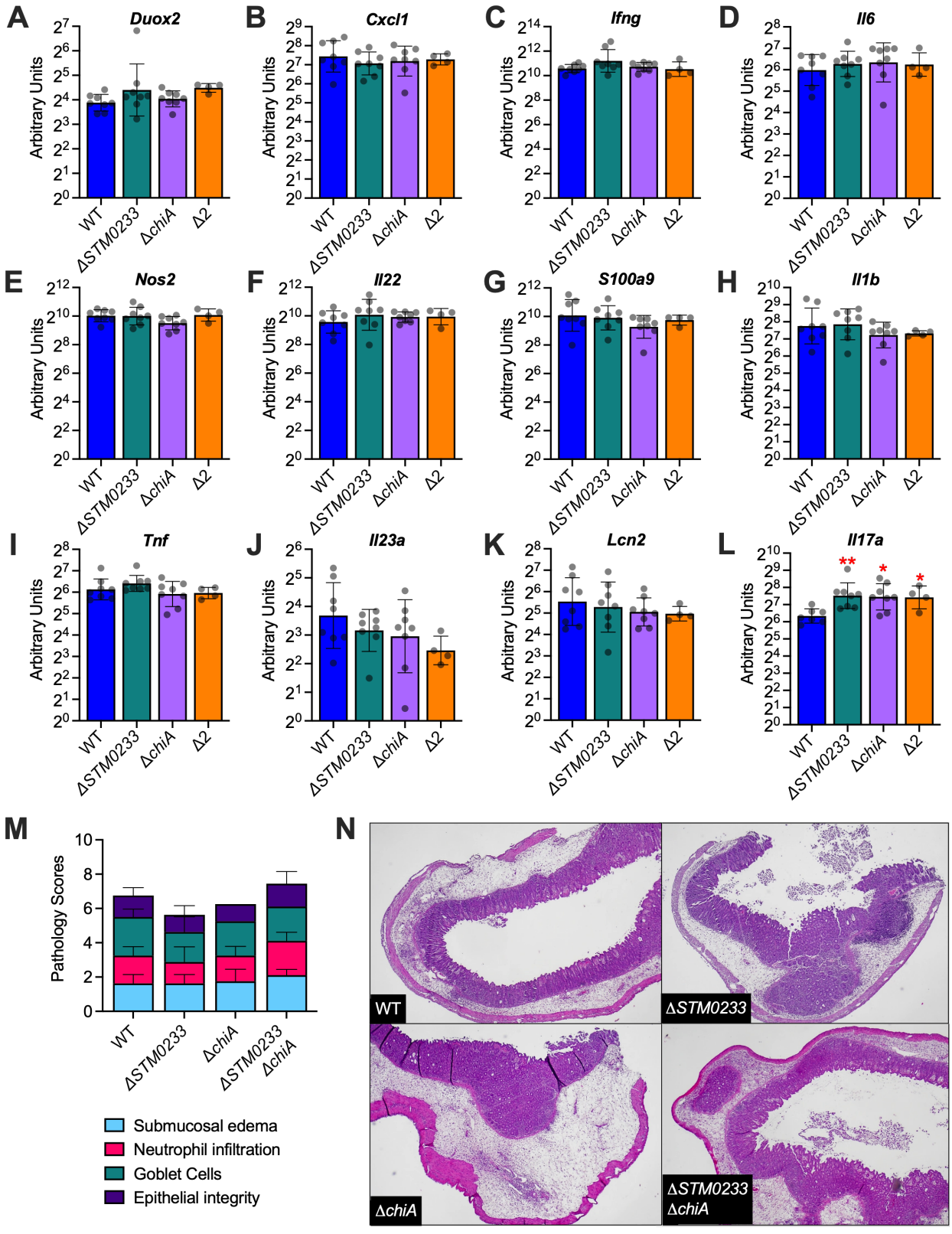

755

Fig. 4. *Salmonella* chitinases do not modulate the innate immune response *in vivo.*

(A-L) mRNA expression of innate immune genes extracted from cecal tissue of *Salmonella* infected mice 48 hpi. Expression is normalized to the housekeeping gene *actb* as well as gene expression in uninfected mice. WT n=8, **Δ***STM0233* n=8, **Δ***chiA* n=8, **Δ***STM0233* **Δ***chiA* n=4. Bars represent geometric mean ± geometric SD. (M) Histopathological scoring of cecal tissue from *Salmonella* infected mice 48 hpi. WT n=8, **Δ***STM0233* n=8, **Δ***chiA* n=8, **Δ***STM0233* **Δ***chiA* n=9. Tissues were scored for submucosal edema, neutrophil infiltration, goblet cells, and epithelial integrity. Bar represents mean ± SD. (N) Representative images of hematoxylin & eosin stained cecal tissue from *Salmonella* infected mice 48 hpi. 400x magnification used for WT and **Δ***STM0233* **Δ***chiA* images, 200x magnification used for **Δ***chiA* and **Δ***STM0233* images. Statistics: (A-M) Stars indicate significance compared to the WT control by one-way ANOVA with Dunnett's multiple comparison test. *=$p<0.05$, **=$p<0.01$.

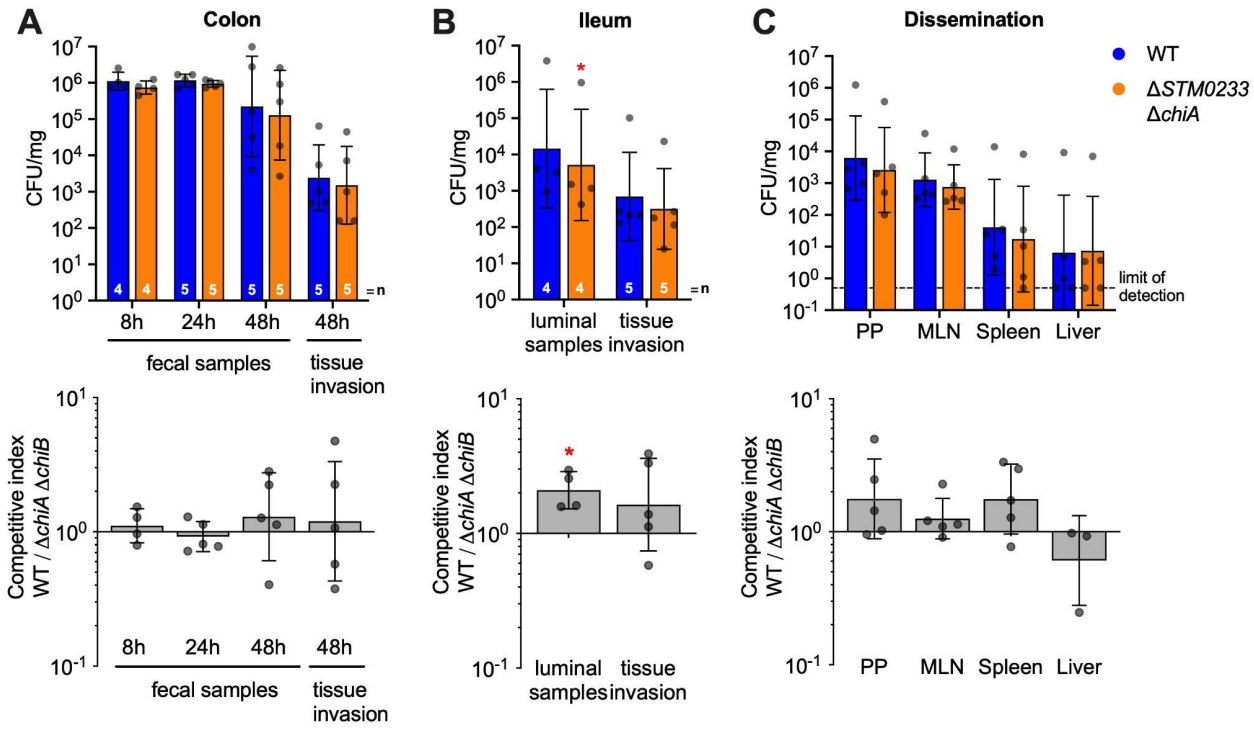

Fig. 5. The presence of WT *Salmonella* rescues the invasion of chitinase-deficient *Salmonella*

Mice infected by oral gavage with a 1:1 ratio of WT and chitinase-deficient *Salmonella*. (A) *Salmonella* colonies recovered from fecal samples collected at 8 and 24 hpi. Fecal samples at 48 hpi were collected directly from the lumen of the colon. Invasion of colonic tissue was determined with a gentamicin protection assay. (B) Luminal samples from the terminal ileum were collected 48 hpi to determine *Salmonella* colonization. Invasion was determined with a gentamicin protection assay performed on the terminal ileum. (C) Colonization of the Peyer's patches (PP), mesenteric lymph nodes (MLN), spleen, and liver 48 h after intragastric infection. n=5. Top panels A-C: CFU/mg recovered for WT and chitinase-deficient *Salmonella*. Bars represent geometric mean ± geometric SD. Bottom panels A-C: the same data expressed as a competitive index, CI= (WT colonization/mutant colonization)/ (WT inoculum/mutant inoculum). Bars represent geometric mean ± geometric SD. Statistics: (Top Row) Paired *t*-test was performed with the

787 absolute values (Bottom Row) the competitive index was analyzed with a one-sample *t*-test
788 against our null hypothesis (competitive index=1). *=p<0.05.
789

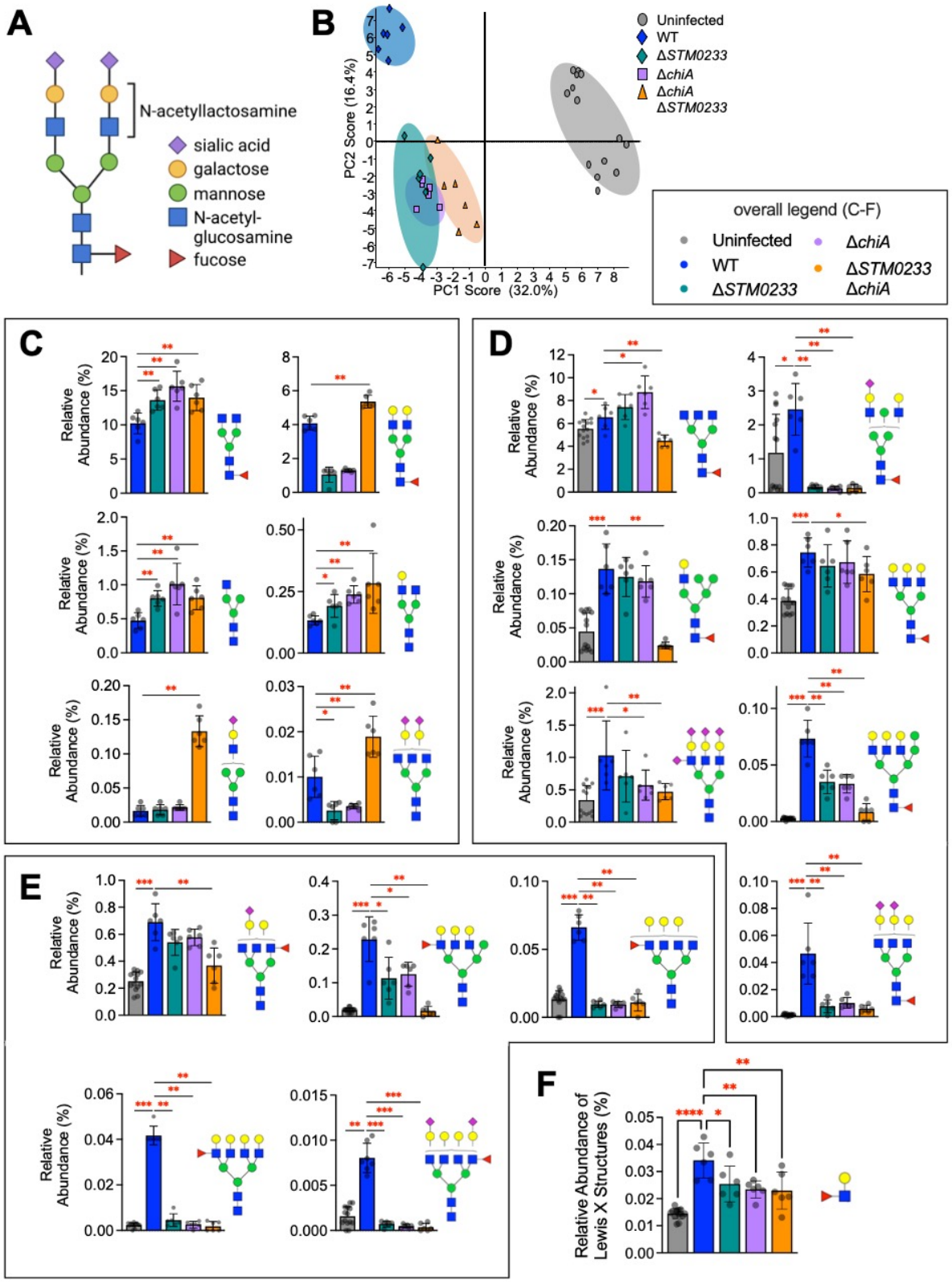

790

Fig. 6. *Salmonella* chitinases induce specific changes in the intestinal glycome during infection.

(A) Common *N*-linked glycan structure. (B) Principal component analysis of the surface glycome composition of uninfected IPEC-1 cells and cells infected with WT *Salmonella* or the chitinase-deficient strains. Uninfected n=14, WT n=6, **Δ***STM0233* n=6, **Δ***chiA* n=6, **Δ***STM0233* **Δ***chiA* n=6. (C) Relative abundance of glycan species that increase during infection with **Δ***STM0233* **Δ***chiA* compared to WT *Salmonella*. (D) Relative abundance of selected glycans species that increase during WT infection compared to uninfected, but do not increase during **Δ***STM0233* **Δ***chiA* infection (E) Relative abundance of selected Lewis X-containing glycans species that increase during WT infection compared to uninfected, but do not increase during **Δ***STM0233* **Δ***chiA* infection. (F) Overall relative abundance of Lewis X structures on all glycans. Bars represent mean ± SD. Statistics: (C-D) Mann-Whitney *U* test (F) One-way ANOVA with Dunnett's multiple comparison test. *=p<0.05, **=p<0.01, ***=p<0.001.

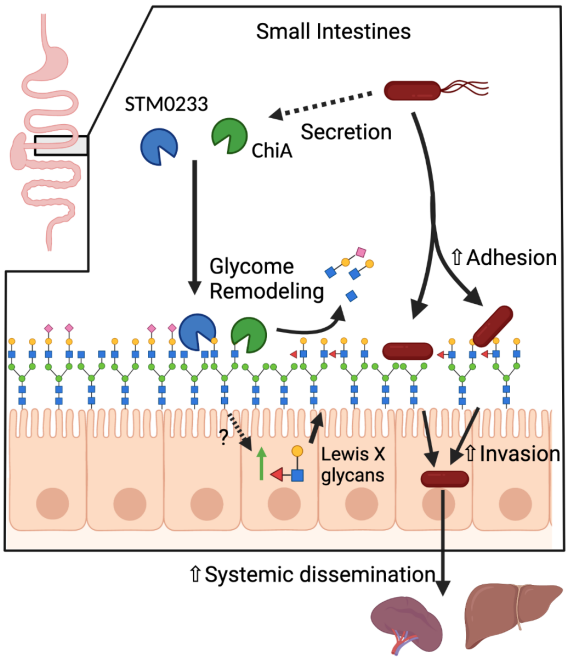

806

807 **Fig. 7. Proposed Model**

808 STM0233 and ChiA are likely secreted into the small intestinal lumen during infection. STM0233
809 and ChiA remodel the surface glycome through the removal of GlcNAc residues of *N*-linked
810 glycans. STM0233 and ChiA also stimulate the upregulation of Lewis X-containing glycans by
811 host cells through an unknown mechanism. STM0233 and ChiA enhance *Salmonella* adhesion
812 to epithelial cells likely due to the exposure of mannose and increase in Lewis X binding residues.
813 Increased adhesion leads to increased invasion of intestinal epithelial cells and increased
814 dissemination to the spleen and liver.

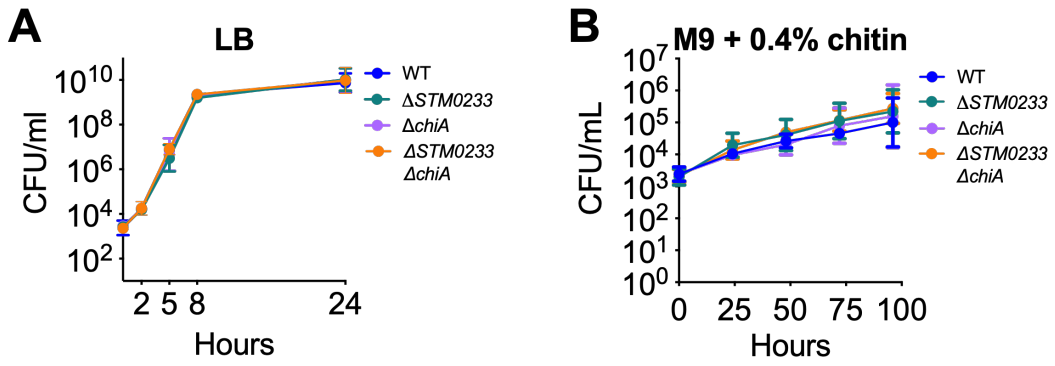

Fig. S1. Deletion of *Salmonella* chitinases does not affect growth characteristics.

(A) Growth of *Salmonella* strains in LB broth at 37 ℃. WT n=5, chitinase-deficient strains n=3. Points represent geometric mean ± geometric SD. (B) Growth of *Salmonella* strains in M9 minimal medium +0.4% colloidal chitin at 37 ℃. n=3. Points represent geometric mean ± geometric SD. Statistics: Mixed-effect analysis and Tukey's multiple comparisons test.

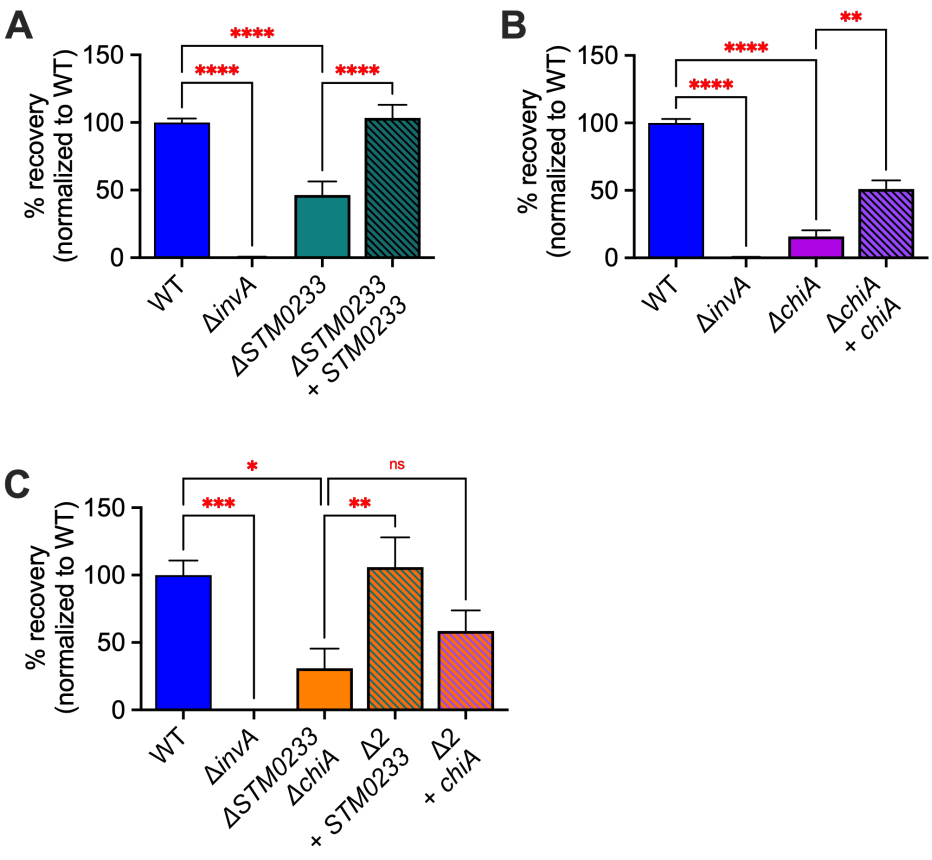

823

824 **Fig. S2. Complementation of chitinase-deficient strains restores invasion.**

825 Chitinase genes were inserted into the Tn7 locus of chitinase-deficient *Salmonella.* Gentamicin
826 protection assay of *Salmonella* infected (MOI:1) small intestinal epithelial cells (IPEC-1). (A)
827 Invasion of **Δ***chiA* and *chiA* complemented strain. n=8. (B) Invasion of **Δ***STM0233* and *STM0233*
828 complemented strain. n=8. (C) Invasion of **Δ***STM0233* **Δ***chiA* (**Δ**2) and **Δ**2 strain complemented
829 with *chiA* or *STM0233*. n=6. Percent recovery of each strain was normalized to WT recovery. Bars
830 represent mean ± SEM. Statistics: One-way ANOVA with Dunnett's multiple comparison test

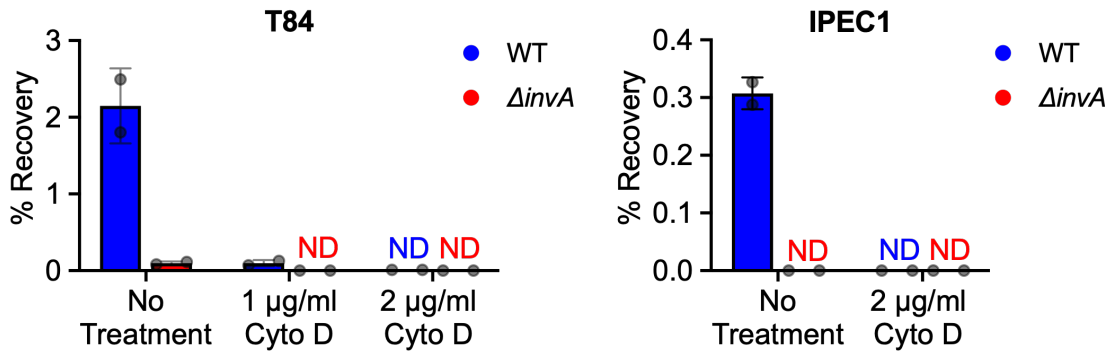

Fig. S3. Cytochalasin D treatment completely blocks *Salmonella* invasion.

(A) Gentamicin protection assay of *Salmonella* infected (MOI:1) colonic epithelial cells (T84) after treatment of epithelial cells with cytochalasin D (1-2 µg/mL). (B) Gentamicin protection assay of *Salmonella* infected (MOI:1) small intestinal epithelial cells (IPEC-1) after treatment of epithelial cells with cytochalasin D (2 µg/mL). n=2. Bars represent mean ± SD.

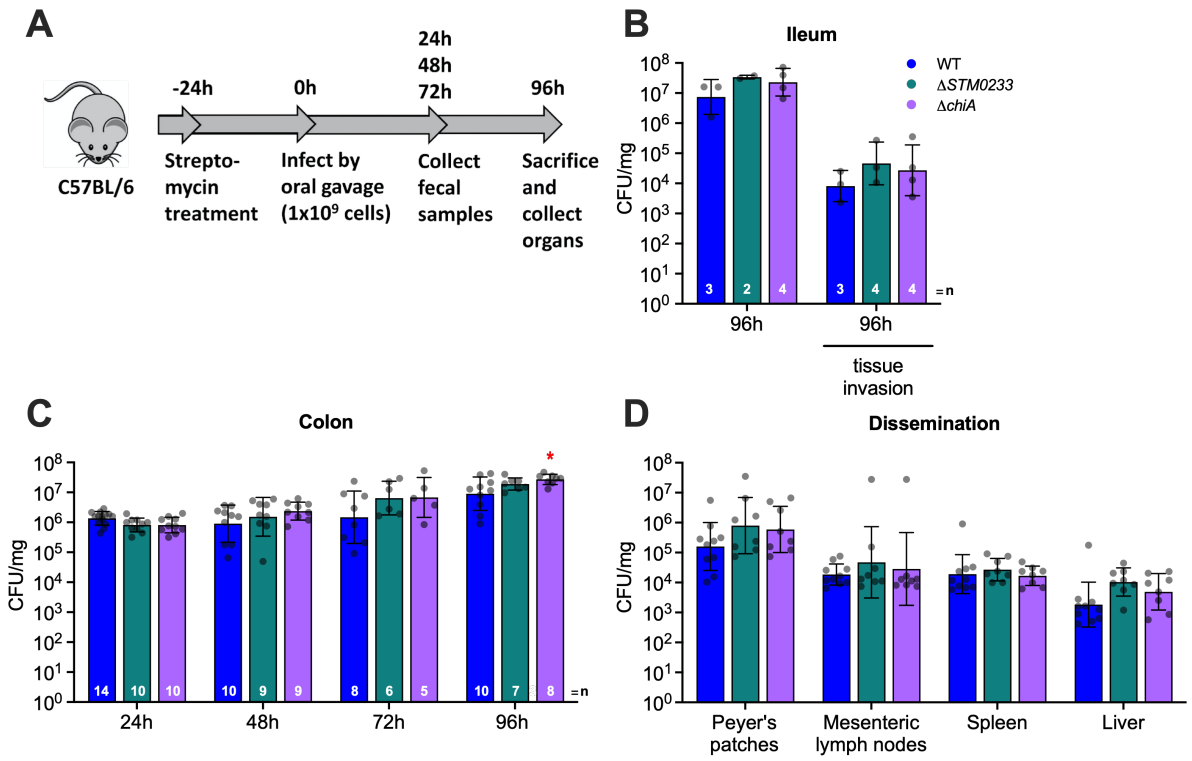

Fig. S4. *Salmonella* chitinases are not required for late-stage infection.

(A) Streptomycin pre-treatment mouse model of 96 h *Salmonella* infection. (B) Luminal samples from the terminal ileum were collected at 96 hpi to determine *Salmonella* colonization. Invasion was determined with a gentamicin protection assay performed on the terminal ileum. WT n=3, **Δ***STM0233* n=3, **Δ***chiA* n=4. (C) *Salmonella* colonies recovered from fecal samples collected at 24, 48, and 72 hpi. Fecal samples at 96 hpi were collected directly from the lumen of the colon. Invasion of colonic tissue was determined with a gentamicin protection assay. WT n=10, **Δ***STM0233* n=8, **Δ***chiA* n=8. (D) Colonization of the Peyer's patches, mesenteric lymph nodes, spleen, and liver after 96 h of intragastric infection. WT n=10, **Δ***STM0233* n=8, **Δ***chiA* n=8. Bars represent geometric mean ± geometric SD. Statistics: (B-D) Stars indicate significance compared to the WT control by one-way ANOVA with Dunnett's multiple comparison test. *=p<0.05.

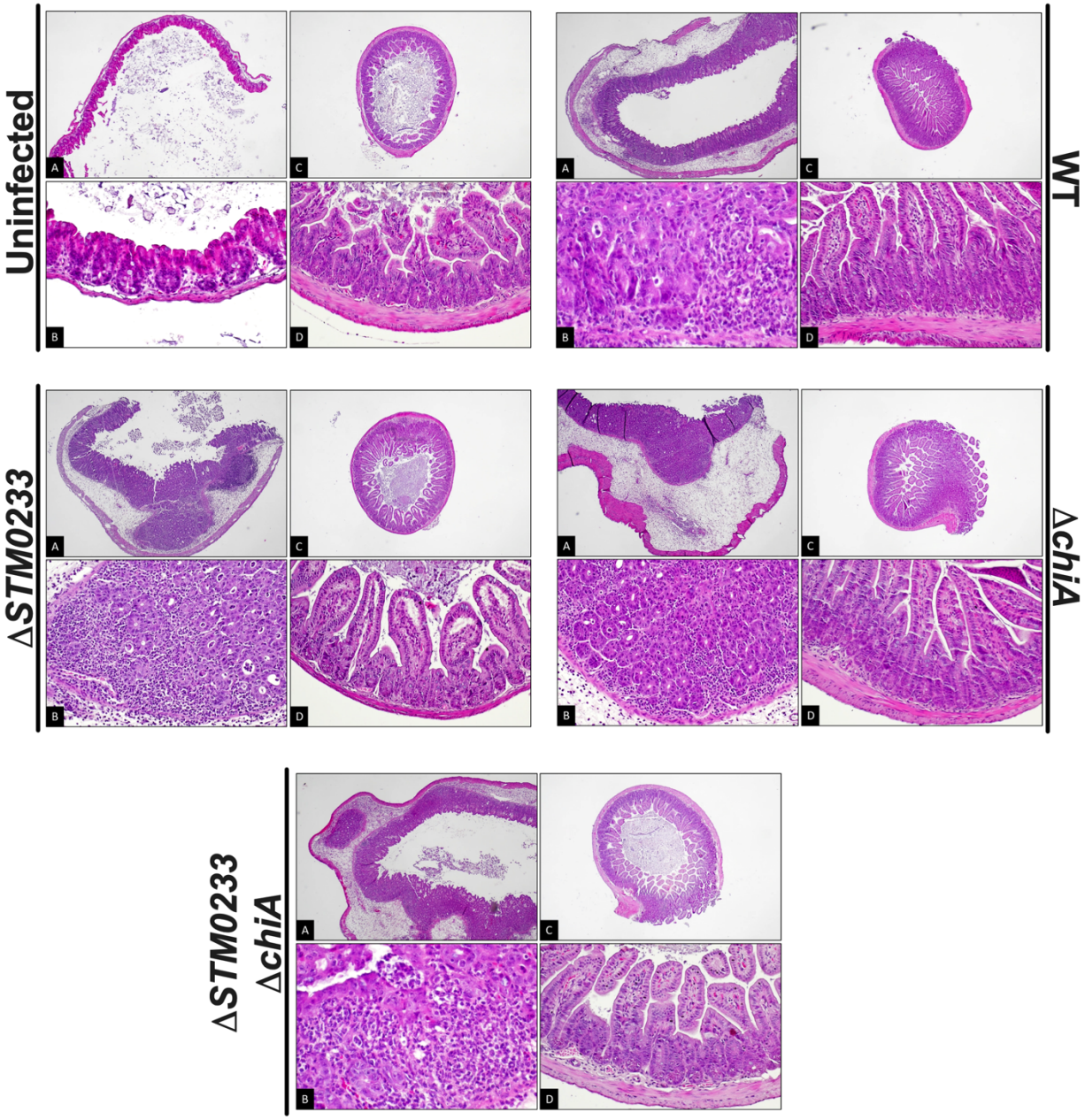

852

853 **Fig. S5. Representative images of cecum and ileum histology.**

854 **Uninfected:** (A) & (B) Cecum – intestine intact without any signs of inflammation [A: low power,
855 hematoxylin eosin, original magnification 40x; B: intermediate power, hematoxylin-eosin, original
856 magnification 200x]. (C) & (D) Ileum – intestine intact without any signs of inflammation [C: low
857 power, hematoxylin eosin, original magnification 40x; D: intermediate power, hematoxylin eosin,
858 original magnification 200x].

WT: (A) & (B) Cecum – moderate inflammation (moderate submucosal edema with lamina propria neutrophilic infiltration with cryptitis, crypt abscess and decrease in goblet cells) [A: low power, hematoxylin-eosin, original magnification 40x; B: high power, hematoxylin-eosin, original magnification 400x]. (C) & (D) Ileum – intestine intact without any signs of inflammation [C: low power, hematoxylin-eosin, original magnification 40x; D: intermediate power, hematoxylin-eosin, original magnification 200x].

Δ*STM0233*: (A) & (B) Cecum – moderate inflammation (moderate submucosal edema with lamina propria neutrophilic infiltration with cryptitis, crypt abscess and decrease in goblet cells) [A: low power, hematoxylin-eosin, original magnification 40x; B: intermediate power, hematoxylin-eosin, original magnification 200x]. (C) & (D) Ileum – intestine intact without any signs of inflammation [C: low power, hematoxylin-eosin, original magnification 40x; D: intermediate power, hematoxylin-eosin, original magnification 200x].

Δ*chiA*: (A) & (B) Cecum – moderate inflammation (profound submucosal edema with lamina propria neutrophilic infiltration with cryptitis, crypt abscess and decrease in goblet cells) [A: low power, hematoxylin-eosin, original magnification 40x; B: intermediate power, hematoxylin-eosin, original magnification 200x]. (C) & (D) Ileum – intestine intact without any signs of inflammation [C: low power, hematoxylin-eosin, original magnification 40x; D: intermediate power, hematoxylin-eosin, original magnification 200x].

Δ*STM0233* Δ*chiA*: (A) & (B) Cecum – moderate inflammation (moderate submucosal edema with lamina propria neutrophilic infiltration with cryptitis, crypt abscess and decrease in goblet cells) [A: low power, hematoxylin-eosin, original magnification 40x; B: high power, hematoxylin- eosin, original magnification 400x]. (C) & (D) Ileum – intestine intact without any signs of inflammation [C: low power, hematoxylin-eosin, original magnification 40x; D: intermediate power, hematoxylin-eosin, original magnification 200x].

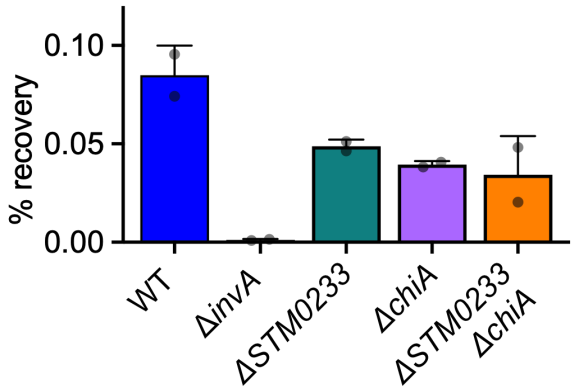

Fig. S6. Chitinase-deficient strains maintained invasion defects for glycome analysis. Gentamicin protection assay of *Salmonella* infected IPEC-1 cells (MOI:1000) done concurrently with infection for the glycome analysis. n=2. Bars represent mean ± SD.

Table S4. Relative abundance of all glycan species identified in glycome analysis. Average relative abundance of glycan species after infecting IPEC-1 cells with *Salmonella* for 1 h (MOI:1000). Uninfected n=14, WT n=6, **Δ***STM0233* n=6, **Δ***chiA* n=6, **Δ***STM0233* **Δ***chiA* n=6. Relative abundance is calculated by dividing glycan species abundance by total glycan abundance. Raw data has been uploaded to GlycoPOST database [39], accession number GPST000225.

References

1. Zhang S, Kingsley RA, Santos RL, Andrews-Polymenis H, Raffatellu M, Figueiredo J, et al. Molecular pathogenesis of Salmonella enterica serotype typhimurium-induced diarrhea. Infect Immun. 2003;71: 1–12. doi:10.1128/IAI.71.1.1-12.2003

2. Knodler LA, Vallance BA, Celli J, Winfree S, Hansen B, Montero M, et al. Dissemination of invasive Salmonella via bacterial-induced extrusion of mucosal epithelia. Proc Natl Acad Sci U S A. 2010;107: 17733–17738. doi:10.1073/pnas.1006098107

3. Gordon MA. Salmonella infections in immunocompromised adults. J Infect. 2008;56: 413–422. doi:10.1016/j.jinf.2008.03.012

4. López FE, de las Mercedes Pescaretti M, Morero R, Delgado MA. Salmonella Typhimurium general virulence factors: A battle of David against Goliath? Food Res Int. 2012;45: 842–851. doi:10.1016/j.foodres.2011.08.009

5. Ibarra JA, Steele-Mortimer O. Salmonella--the ultimate insider. Salmonella virulence factors that modulate intracellular survival. Cell Microbiol. 2009;11: 1579–1586. doi:10.1111/j.1462-5822.2009.01368.x

6. Broz P, Ohlson MB, Monack DM. Innate immune response to Salmonella typhimurium, a model enteric pathogen. Gut Microbes. 2012;3: 62–70. doi:10.4161/gmic.19141

7. Arabyan N, Huang BC, Weimer BC. Draft Genome Sequences of Salmonella enterica Serovar Typhimurium LT2 with Deleted Chitinases That Are Emerging Virulence Factors. Genome Announc. 2017;5. doi:10.1128/genomeA.00659-17

8. Hamid R, Khan MA, Ahmad M, Ahmad MM, Abdin MZ, Musarrat J, et al. Chitinases: An update. J Pharm Bioallied Sci. 2013;5: 21–29. doi:10.4103/0975-7406.106559

9. Bokma E, van Koningsveld GA, Jeronimus-Stratingh M, Beintema JJ. Hevamine, a chitinase from the rubber treeHevea brasiliensis, cleaves peptidoglycan between the C-1 ofN-acetylglucosamine and C-4 ofN-acetylmuramic acid and therefore is not a lysozyme. FEBS Letters. 1997. pp. 161–163. doi:10.1016/s0014-5793(97)00682-0

10. Rehman S, Grigoryeva LS, Richardson KH, Corsini P, White RC, Shaw R, et al. Structure and functional analysis of the Legionella pneumophila chitinase ChiA reveals a novel mechanism of metal-dependent mucin degradation. PLoS Pathog. 2020;16: e1008342. doi:10.1371/journal.ppat.1008342

11. DebRoy S, Dao J, Söderberg M, Rossier O, Cianciotto NP. Legionella pneumophila type II secretome reveals unique exoproteins and a chitinase that promotes bacterial persistence in the lung. Proc Natl Acad Sci U S A. 2006;103: 19146–19151. doi:10.1073/pnas.0608279103

12. Chaudhuri S, Gantner BN, Ye RD, Cianciotto NP, Freitag NE. The Listeria monocytogenes ChiA chitinase enhances virulence through suppression of host innate immunity. MBio. 2013;4: e00617-12. doi:10.1128/mBio.00617-12

13. Chaudhuri S, Bruno JC, Alonzo F, Xayarath B, Cianciotto NP, Freitag NE. Contribution of Chitinases to Listeria monocytogenes Pathogenesis. Applied and Environmental Microbiology. 2010. pp. 7302–7305. doi:10.1128/aem.01338-10

14. Mondal M, Nag D, Koley H, Saha DR, Chatterjee NS. The Vibrio cholerae extracellular chitinase ChiA2 is important for survival and pathogenesis in the host intestine. PLoS One. 2014;9: e103119. doi:10.1371/journal.pone.0103119

15. Bhowmick R, Ghosal A, Das B, Koley H, Saha DR, Ganguly S, et al. Intestinal adherence of Vibrio cholerae involves a coordinated interaction between colonization factor GbpA and mucin. Infect Immun. 2008;76: 4968–4977. doi:10.1128/IAI.01615-07

16. Low D, Tran HT, Lee I-A, Dreux N, Kamba A, Reinecker H-C, et al. Chitin-binding domains of Escherichia coli ChiA mediate interactions with intestinal epithelial cells in mice with colitis. Gastroenterology. 2013;145: 602–12.e9. doi:10.1053/j.gastro.2013.05.017

17. Kawada M, Chen C-C, Arihiro A, Nagatani K, Watanabe T, Mizoguchi E. Chitinase 3-like-1 enhances bacterial adhesion to colonic epithelial cells through the interaction with bacterial chitin-binding protein. Laboratory Investigation. 2008. pp. 883–895. doi:10.1038/labinvest.2008.47

18. Mizoguchi E. Chitinase 3-like-1 exacerbates intestinal inflammation by enhancing bacterial adhesion and invasion in colonic epithelial cells. Gastroenterology. 2006;130: 398–411. doi:10.1053/j.gastro.2005.12.007

19. Hautefort I, Thompson A, Eriksson-Ygberg S, Parker ML, Lucchini S, Danino V, et al. During infection of epithelial cells Salmonella enterica serovar Typhimurium undergoes a time-dependent transcriptional adaptation that results in simultaneous expression of three type 3 secretion systems. Cell Microbiol. 2008;10: 958–984. doi:10.1111/j.1462-5822.2007.01099.x

20. Eriksson S, Lucchini S, Thompson A, Rhen M, Hinton JCD. Unravelling the biology of macrophage infection by gene expression profiling of intracellular Salmonella enterica. Mol Microbiol. 2003;47: 103–118. doi:10.1046/j.1365-2958.2003.03313.x

21. Harvey PC, Watson M, Hulme S, Jones MA, Lovell M, Berchieri A Jr, et al. Salmonella enterica serovar typhimurium colonizing the lumen of the chicken intestine grows slowly and upregulates a unique set of virulence and metabolism genes. Infect Immun. 2011;79: 4105–4121. doi:10.1128/IAI.01390-10

22. Larsen T, Petersen BO, Storgaard BG, Duus JØ, Palcic MM, Leisner JJ. Characterization of a novel Salmonella Typhimurium chitinase which hydrolyzes chitin, chitooligosaccharides and an N-acetyllactosamine conjugate. Glycobiology. 2011;21: 426–436. doi:10.1093/glycob/cwq174

23. Frederiksen RF, Yoshimura Y, Storgaard BG, Paspaliari DK, Petersen BO, Chen K, et al. A Diverse Range of Bacterial and Eukaryotic Chitinases Hydrolyzes the LacNAc (Galβ1–4GlcNAc) and LacdiNAc (GalNAcβ1–4GlcNAc) Motifs Found on Vertebrate and Insect Cells. Journal of Biological Chemistry. 2015. pp. 5354–5366. doi:10.1074/jbc.m114.607291

24. Kavanaugh D, O'Callaghan J, Kilcoyne M, Kane M, Joshi L, Hickey RM. The intestinal glycome and its modulation by diet and nutrition. Nutr Rev. 2015;73: 359–375. doi:10.1093/nutrit/nuu019

25. Arabyan N, Park D, Foutouhi S, Weis AM, Huang BC, Williams CC, et al. Salmonella Degrades the Host Glycocalyx Leading to Altered Infection and Glycan Remodeling. Scientific Reports. 2016. doi:10.1038/srep29525

26. Park D, Arabyan N, Williams CC, Song T, Mitra A, Weimer BC, et al. Salmonella typhimurium enzymatically landscapes the host intestinal epithelial cell (IEC) surface glycome to increase invasion. Mol Cell Proteomics. 2016;15: 3653–3664. doi:10.1074/mcp.m116.063206

27. Thankavel K, Shah AH, Cohen MS, Ikeda T, Lorenz RG, Curtiss R 3rd, et al. Molecular

basis for the enterocyte tropism exhibited by Salmonella typhimurium type 1 fimbriae. J Biol Chem. 1999;274: 5797–5809. doi:10.1074/jbc.274.9.5797

28. Galán JE, Curtiss R 3rd. Cloning and molecular characterization of genes whose products allow Salmonella typhimurium to penetrate tissue culture cells. Proc Natl Acad Sci U S A. 1989;86: 6383–6387. doi:10.1073/pnas.86.16.6383

29. Lou L, Zhang P, Piao R, Wang Y. Salmonella Pathogenicity Island 1 (SPI-1) and Its Complex Regulatory Network. Front Cell Infect Microbiol. 2019;9: 270. doi:10.3389/fcimb.2019.00270

30. Wagner C, Hensel M. Adhesive mechanisms of Salmonella enterica. Adv Exp Med Biol. 2011;715: 17–34. doi:10.1007/978-94-007-0940-9_2

31. Lara-Tejero M, Galán JE. Salmonella enterica serovar typhimurium pathogenicity island 1-encoded type III secretion system translocases mediate intimate attachment to nonphagocytic cells. Infect Immun. 2009;77: 2635–2642. doi:10.1128/IAI.00077-09

32. Misselwitz B, Kreibich SK, Rout S, Stecher B, Periaswamy B, Hardt W-D. Salmonella enterica serovar Typhimurium binds to HeLa cells via Fim-mediated reversible adhesion and irreversible type three secretion system 1-mediated docking. Infect Immun. 2011;79: 330–341. doi:10.1128/IAI.00581-10

33. Barthel M, Hapfelmeier S, Quintanilla-Martínez L, Kremer M, Rohde M, Hogardt M, et al. Pretreatment of mice with streptomycin provides a Salmonella enterica serovar Typhimurium colitis model that allows analysis of both pathogen and host. Infect Immun. 2003;71: 2839–2858. doi:10.1128/iai.71.5.2839-2858.2003

34. Jepson MA, Clark MA. The role of M cells in Salmonella infection. Microbes Infect. 2001;3: 1183–1190. doi:10.1016/s1286-4579(01)01478-2

35. Watson KG, Holden DW. Dynamics of growth and dissemination of Salmonella in vivo. Cell Microbiol. 2010;12: 1389–1397. doi:10.1111/j.1462-5822.2010.01511.x

36. Hurley D, McCusker MP, Fanning S, Martins M. Salmonella-host interactions - modulation of the host innate immune system. Front Immunol. 2014;5: 481. doi:10.3389/fimmu.2014.00481

37. Almagro Armenteros JJ, Tsirigos KD, Sønderby CK, Petersen TN, Winther O, Brunak S, et al. SignalP 5.0 improves signal peptide predictions using deep neural networks. Nat Biotechnol. 2019;37: 420–423. doi:10.1038/s41587-019-0036-z

38. Bendtsen JD, Kiemer L, Fausbøll A, Brunak S. Non-classical protein secretion in bacteria. BMC Microbiol. 2005;5: 58. doi:10.1186/1471-2180-5-58

39. Watanabe Y, Aoki-Kinoshita KF, Ishihama Y, Okuda S. GlycoPOST realizes FAIR principles for glycomics mass spectrometry data. Nucleic Acids Res. 2021;49: D1523–D1528. doi:10.1093/nar/gkaa1012

40. Tran HT, Barnich N, Mizoguchi E. Potential role of chitinases and chitin-binding proteins in host-microbial interactions during the development of intestinal inflammation. Histol Histopathol. 2011;26: 1453–1464. doi:10.14670/HH-26.1453

41. Frederiksen RF, Leisner JJ. Effects of Listeria monocytogenes EGD-e and Salmonella enterica ser. Typhimurium LT2 chitinases on intracellular survival in Dictyostelium discoideum and mammalian cell lines. FEMS Microbiol Lett. 2015;362. doi:10.1093/femsle/fnv067

42. Kirn TJ, Jude BA, Taylor RK. A colonization factor links Vibrio cholerae environmental survival and human infection. Nature. 2005;438: 863–866. doi:10.1038/nature04249

43. Bäumler AJ, Tsolis RM, Heffron F. Contribution of fimbrial operons to attachment to and invasion of epithelial cell lines by Salmonella typhimurium. Infect Immun. 1996;64: 1862–1865. doi:10.1128/iai.64.5.1862-1865.1996

44. Bäumler AJ, Tsolis RM, Bowe FA, Kusters JG, Hoffmann S, Heffron F. The pef fimbrial operon of Salmonella typhimurium mediates adhesion to murine small intestine and is necessary for fluid accumulation in the infant mouse. Infect Immun. 1996;64: 61–68. doi:10.1128/iai.64.1.61-68.1996

45. Costa J, Ahluwalia A. Advances and Current Challenges in Intestinal Model Engineering: A Digest. Front Bioeng Biotechnol. 2019;7: 144. doi:10.3389/fbioe.2019.00144

46. Sonnenburg JL, Xu J, Leip DD, Chen C-H, Westover BP, Weatherford J, et al. Glycan foraging in vivo by an intestine-adapted bacterial symbiont. Science. 2005;307: 1955–1959. doi:10.1126/science.1109051

47. Pickard JM, Maurice CF, Kinnebrew MA, Abt MC, Schenten D, Golovkina TV, et al. Rapid fucosylation of intestinal epithelium sustains host–commensal symbiosis in sickness. Nature. 2014;514: 638–641. doi:10.1038/nature13823

48. Renkema GH, Herma Renkema G, Boot RG, Au FL, Donker-Koopman WE, Strijland A, et al. Chitotriosidase, a chitinase, and the 39-kDa human cartilage glycoprotein, a chitin-binding lectin, are homologues of family 18 glycosyl hydrolases secreted by human macrophages. European Journal of Biochemistry. 1998. pp. 504–509. doi:10.1046/j.1432-1327.1998.2510504.x

49. Aomatsu T, Imaeda H, Matsumoto K, Kimura E, Yoden A, Tamai H, et al. Faecal chitinase 3-like-1: a novel biomarker of disease activity in paediatric inflammatory bowel disease. Alimentary Pharmacology & Therapeutics. 2011. pp. 941–948. doi:10.1111/j.1365-2036.2011.04805.x

50. Buisson A, Vazeille E, Minet-Quinard R, Goutte M, Bouvier D, Goutorbe F, et al. Faecal chitinase 3-like 1 is a reliable marker as accurate as faecal calprotectin in detecting endoscopic activity in adult patients with inflammatory bowel diseases. Aliment Pharmacol Ther. 2016;43: 1069–1079. doi:10.1111/apt.13585

51. Arabyan N, Weis AM, Huang BC, Weimer BC. Implication of Sialidases in Infection: Genome Release of Sialidase Knockout Strains from Serovar Typhimurium LT2. Genome Announc. 2017;5. doi:10.1128/genomeA.00341-17

52. Hase K, Kawano K, Nochi T, Pontes GS, Fukuda S, Ebisawa M, et al. Uptake through glycoprotein 2 of FimH bacteria by M cells initiates mucosal immune response. Nature. 2009. pp. 226–230. doi:10.1038/nature08529

53. Kolenda R, Burdukiewicz M, Schiebel J, Rödiger S, Sauer L, Szabo I, et al. Adhesion of Salmonella to Pancreatic Secretory Granule Membrane Major Glycoprotein GP2 of Human and Porcine Origin Depends on FimH Sequence Variation. Frontiers in Microbiology. 2018. doi:10.3389/fmicb.2018.01905

54. Chessa D, Dorsey CW, Winter M, Baümler AJ. Binding specificity of Salmonella plasmid-encoded fimbriae assessed by glycomics. J Biol Chem. 2008;283: 8118–8124. doi:10.1074/jbc.M710095200

55. Stojiljkovic I, Bäumler AJ, Heffron F. Ethanolamine utilization in Salmonella typhimurium: nucleotide sequence, protein expression, and mutational analysis of the cchA cchB eutE eutJ eutG eutH gene cluster. J Bacteriol. 1995;177: 1357–1366. doi:10.1128/jb.177.5.1357-1366.1995

56. de Lorenzo V, Cases I, Herrero M, Timmis KN. Early and late responses of TOL promoters to pathway inducers: identification of postexponential promoters in Pseudomonas putida with lacZ-tet bicistronic reporters. J Bacteriol. 1993;175: 6902–6907. doi:10.1128/jb.175.21.6902-6907.1993

57. Schmieger H. Phage P22-mutants with increased or decreased transduction abilities. Mol Gen Genet. 1972;119: 75–88. doi:10.1007/BF00270447

58. Schmieger H. The molecular structure of the transducing particles of Salmonella phage P22. II. Density gradient analysis of DNA. Mol Gen Genet. 1970;109: 323–337. doi:10.1007/BF00267702

59. Miller VL, Mekalanos JJ. A novel suicide vector and its use in construction of insertion mutations: osmoregulation of outer membrane proteins and virulence determinants in Vibrio cholerae requires toxR. J Bacteriol. 1988;170: 2575–2583. doi:10.1128/jb.170.6.2575-2583.1988

60. Prentki P, Krisch HM. In vitro insertional mutagenesis with a selectable DNA fragment. Gene. 1984;29: 303–313. doi:10.1016/0378-1119(84)90059-3

61. Datsenko KA, Wanner BL. One-step inactivation of chromosomal genes in Escherichia coli K-12 using PCR products. Proceedings of the National Academy of Sciences. 2000. pp. 6640–6645. doi:10.1073/pnas.120163297

62. McKenzie GJ, Craig NL. Fast, easy and efficient: site-specific insertion of transgenes into enterobacterial chromosomes using Tn7 without need for selection of the insertion event. BMC Microbiol. 2006;6: 39. doi:10.1186/1471-2180-6-39

63. Elhadad D, Desai P, Grassl GA, McClelland M, Rahav G, Gal-Mor O. Differences in Host Cell Invasion and Salmonella Pathogenicity Island 1 Expression between Salmonella enterica Serovar Paratyphi A and Nontyphoidal S . Typhimurium. Infection and Immunity. 2016. pp. 1150–1165. doi:10.1128/iai.01461-15

64. Murthy N, Bleakley B. Simplified method of preparing colloidal chitin used for screening of chitinase-producing microorganisms. Internet J Microbiol. 2012;10: e2bc3. Available: https://print.ispub.com/api/0/ispub-article/14186

65. Botteldoorn N, Van Coillie E, Grijspeerdt K, Werbrouck H, Haesebrouck F, Donné E, et al.

Real-time reverse transcription PCR for the quantification of the mntH expression of Salmonella enterica as a function of growth phase and phagosome-like conditions. J Microbiol Methods. 2006;66: 125–135. doi:10.1016/j.mimet.2005.11.003

66. Behnsen J, Jellbauer S, Wong CP, Edwards RA, George MD, Ouyang W, et al. The cytokine IL-22 promotes pathogen colonization by suppressing related commensal bacteria. Immunity. 2014;40: 262–273. doi:10.1016/j.immuni.2014.01.003

67. Hamers AAJ, Uleman S, van Tiel CM, Kruijswijk D, van Stalborch A-M, Huveneers S, et al. Limited role of nuclear receptor Nur77 in Escherichia coli-induced peritonitis. Infect Immun. 2014;82: 253–264. doi:10.1128/IAI.00721-13

68. Spandidos A, Wang X, Wang H, Seed B. PrimerBank: a resource of human and mouse PCR primer pairs for gene expression detection and quantification. Nucleic Acids Res. 2010;38: D792-9. doi:10.1093/nar/gkp1005

69. Aquilano K, Ceci V, Gismondi A, De Stefano S, Iacovelli F, Faraonio R, et al. Adipocyte metabolism is improved by TNF receptor-targeting small RNAs identified from dried nuts. Communications Biology. 2019. doi:10.1038/s42003-019-0563-7

70. Dong X, Zhou S, Mechref Y. LC-MS/MS analysis of permethylated free oligosaccharides and N-glycans derived from human, bovine, and goat milk samples. Electrophoresis. 2016;37: 1532–1548. doi:10.1002/elps.201500561

71. Gautam S, Peng W, Cho BG, Huang Y, Banazadeh A, Yu A, et al. Glucose unit index (GUI) of permethylated glycans for effective identification of glycans and glycan isomers. Analyst. 2020;145: 6656–6667. doi:10.1039/d0an00314j

72. Peng W, Goli M, Mirzaei P, Mechref Y. Revealing the Biological Attributes of N-Glycan Isomers in Breast Cancer Brain Metastasis Using Porous Graphitic Carbon (PGC) Liquid Chromatography-Tandem Mass Spectrometry (LC-MS/MS). J Proteome Res. 2019;18: 3731–3740. doi:10.1021/acs.jproteome.9b00429

73. Yu C-Y, Mayampurath A, Hu Y, Zhou S, Mechref Y, Tang H. Automated annotation and quantification of glycans using liquid chromatography-mass spectrometry. Bioinformatics. 2013;29: 1706–1707. doi:10.1093/bioinformatics/btt190